[14] Murphy D, Detjen KM, Welzel M, Wiedenmann B, Rosewicz S. Interferon-alpha delays S-phase progression in human hepatocellular carcinoma cells via inhibition of specific cyclin-dependent kinases. Hepatology 2001;33:346–356.
[15] Obora A, Shiratori Y, Okuno M, Adachi S, Takano Y, Matsushima-Nishiwaki R, et al. Synergistic induction of apoptosis by acyclic retinoid and interferon-beta in human hepatocellular carcinoma cells. Hepatology 2002;36:1115–1124.
[16] Eguchi H, Nagano H, Yamamoto H, Miyamoto A, Kondo M, Dono K, et al. Augmentation of antitumor activity of 5-fluorouracil by interferon alpha is associated with up-regulation of p27Kip1 in human hepatocellular carcinoma cells. Clin Cancer Res 2000;6:2881–2890.
[17] Radaeva S, Jaruga B, Hong F, Kim WH, Fan S, Cai H, et al. Interferon-alpha activates multiple STAT signals and down-regulates c-Met in primary human hepatocytes. Gastroenterology 2002;122:1020–1034.
[18] Ikeda K, Arase Y, Saitoh S, Kobayashi M, Suzuki Y, Suzuki F, et al. Interferon beta prevents recurrence of hepatocellular carcinoma after complete resection or ablation of the primary tumor-A prospective randomized study of hepatitis C virus-related liver cancer. Hepatology 2000;32:228–232.
[19] Borden EC, Hogan TF, Voelkel JG. Comparative antiproliferative activity in vitro of natural interferons alpha and beta for diploid and transformed human cells. Cancer Res 1982;42:4948–4953.
[20] Johns TG, Mackay IR, Callister KA, Hertzog PJ, Devenish RJ, Linnane AW. Antiproliferative potencies of interferons on melanoma cell lines and xenografts: higher efficacy of interferon beta. J Natl Cancer Inst 1992;84:1185–1190.
[21] Damdinsuren B, Nagano H, Sakon M, Kondo M, Yamamoto T, Umeshita K, et al. Interferon-beta is more potent than interferon-alpha in inhibition of human hepatocellular carcinoma cell growth when used alone and in combination with anticancer drugs. Ann Surg Oncol 2003;10:1184–1190.
[22] Murata M, Nabeshima S, Kikuchi K, Yamaji K, Furusyo N, Hayashi J. A comparison of the antitumor effects of interferon-alpha and beta on human hepatocellular carcinoma cell lines. Cytokine 2006;33:121–128.
[23] Damdinsuren B, Nagano H, Wada H, Kondo M, Ota H, Nakamura M, et al. Stronger growth-inhibitory effect of interferon (IFN)-beta compared to IFN-alpha is mediated by IFN signaling pathway in hepatocellular carcinoma cells. Int J Oncol 2007;30:201–208.
[24] Kim CM, Koike K, Saito I, Miyamura T, Jay G. HBx gene of hepatitis B virus induces liver cancer in transgenic mice. Nature 1991;351:317–320.
[25] Koike K, Moriya K, Iino S, Yotsuyanagi H, Endo Y, Miyamura T, et al. High-level expression of hepatitis B virus HBx gene and hepatocarcinogenesis in transgenic mice. Hepatology 1994;19:810–819.
[26] Koike K, Moriya K, Yotsuyanagi H, Shintani Y, Fujie H, Tsutsumi T, et al. Compensatory apoptosis in preneoplastic liver of a transgenic mouse model for viral hepatocarcinogenesis. Cancer Lett 1998;134:181–186.
[27] Merle P, Chevallier M, Levy R, Maisonnas M, Terradillos O, Si Ahmed SN, et al. Preliminary results of interferon-alpha therapy on woodchuck hepatitis virus-induced hepatocarcinogenesis: possible benefit in female transgenic mice. J Hepatol 2001;34:562–569.
[28] Merle P, Barraud L, Lefrancois L, Chevallier M, Guerret S, Maisonnas M, et al. Long-term high-dose interferon-alpha therapy delays Hepadnavirus-related hepatocarcinogenesis in X/myc transgenic mice. Oncogene 2003;22:2762–2771.
[29] Nakaji M, Yano Y, Ninomiya T, Seo Y, Hamano K, Yoon S, et al. IFN-alpha prevents the growth of pre-neoplastic lesions and inhibits the development of hepatocellular carcinoma in the rat. Carcinogenesis 2004;25:389–397.
[30] Matsuyama S, Henmi S, Ichihara N, Sone S, Kikuchi T, Ariga T, et al. Protective effects of murine recombinant interferon-β administered by intravenous, intramuscular or subcutaneous route on mouse hepatitis virus infection. Antiviral Res 2000;47:131–137.
[31] Ton TT, Foley JF, Flagler ND, Gaul BW, Maronpot RR. Feasibility of administering 5-bromo-2′-deoxyuridine (BRDU) in drinking water for labeling S-phase hepatocytes in mice and rats. Toxicol Methods 1997;7:123–136.
[32] Seglen PO. Preparation of rat liver cells: enzymatic requirements for tissue dispersion. Exp Cell Res 1991;2:391–398.
[33] Soriano HE, Kang DC, Finegold MJ, Hicks MJ, Wang ND, Harrison W, et al. Lack of C/EBP alpha gene expression results in increased DNA synthesis and an increased frequency of immortalization of freshly isolated mice [correction of rat] hepatocytes. Hepatology 1998;27:392–401.
[34] Sugiyama N, Mizuguchi T, Aoki T, Hui T, Inderbitzin D, Demetriou AA, et al. Glycerol suppresses proliferation of rat hepatocytes and human HepG2 cells. J Surg Res 2002;103:236–242.
[35] Bucio L, Souza V, Gomez JJ, Campos C, Carabez A. Expression of some hepatocyte-like functional properties of WRL-68 cells in culture. In Vitro Cell Dev Biol Anim 1994;30A:366–371.
[36] Begg AC, McNally NJ, Shrieve DC, Karcher H. A method to measure the duration of DNA synthesis and the potential doubling time from a single sample. Cytometry 1985;6:620–626.
[37] Dolbeare F, Selden JR. Immunochemical quantitation of bromodeoxyuridine: application to cell-cycle kinetics. Methods in cell biology, vol. 41. Academic Press, Inc.; 1994. p. 297–315.
[38] Seki Y, Toba K, Fuse I, Sato N, Niwano H, Takahashi H, et al. In vitro effect of cyclosporin A, mitomycin C and prednisolone on cell kinetics in cultured human umbilical vein endothelial cells. Thromb Res 2005;115:219–228.
[39] Sato R, Maesawa C, Fujisawa K, Wada K, Oikawa K, Takikawa Y, et al. Prevention of critical telomere shortening by oestradiol in human normal hepatic cultured cells and carbon tetrachloride induced rat liver fibrosis. Gut 2004;53:1001–1009.
[40] Bromberg JF, Fan Z, Brown C, Mendelsohn J, Darnell Jr JE. Epidermal growth factor-induced growth inhibition requires Stat1 activation. Cell Growth Differ 1998;9:505–512.
[41] Chin YE, Kitagawa M, Su WC, You ZH, Iwamoto Y, Fu XY. Cell growth arrest and induction of cyclin-dependent kinase inhibitor p21 WAF1/CIP1 mediated by STAT1. Science 1996;272:719–722.
[42] Bromberg JF, Wrzeszczynska MH, Devgan G, Zhao Y, Pestell RG, Albanese C, et al. Stat3 as an oncogene. Cell 1999;98:295–303.
[43] Song JI, Rubin Grandis J. STAT signaling in head and neck cancer. Oncogene 2000;19:2489–2495.
[44] Inamura K, Matsuzaki Y, Uematsu N, Honda A, Tanaka N, Uchida K. Rapid inhibition of MAPK signaling and anti-proliferation effect via JAK/STAT signaling by interferon-alpha in hepatocellular carcinoma cell lines. Biochim Biophys Acta 2005;1745:401–410.
[45] Ruff-Jamison S, Chen K, Cohen S. Induction by EGF and interferon-gamma of tyrosine phosphorylated DNA binding proteins in mouse liver nuclei. Science 1993;261:1733–1736.
[46] Ruff-Jamison S, Zhong Z, Wen Z, Chen K, Darnell Jr JE, Cohen S. Epidermal growth factor and lipopolysaccharide activate Stat3 transcription factor in mouse liver. J Biol Chem 1994;269:21933–21935.

Available online at www.sciencedirect.com
ScienceDirect
Biochemical and Biophysical Research Communications 365 (2008) 595–601
BBRC
www.elsevier.com/locate/ybbrc

Sca-1+ endothelial cells (SPECs) reside in the portal area of the liver and contribute to rapid recovery from acute liver disease ☆

Atsunori Tsuchiya [a,b], Toshio Heike [a], Shiro Baba [a], Hisanori Fujino [a], Katsutsugu Umeda [a], Yasunobu Matsuda [b], Minoru Nomoto [b], Takafumi Ichida [c], Yutaka Aoyagi [b], Tatsutoshi Nakahata [a,*]

[a] *Department of Pediatrics, Graduate School of Medicine, Kyoto University, 54 Kawara-cho, Shogoin, Sakyo-ku, Kyoto 606-8507, Japan*
[b] *Division of Gastroenterology and Hepatology, Graduate School of Medical and Dental Science, Niigata University, Asahimachi-Dori-1 Bancho 757, Chuo-Ku, Niigata 951-8510, Japan*
[c] *Department of Gastroenterology, Juntendo University School of Medicine, 1129 Nagaoka, Izunokuni 410-2295, Japan*

Received 10 October 2007
Available online 5 November 2007

Abstract

The liver has a high potential to regenerate however, the relation between oval cells and endothelial cells in the portal area during liver regeneration has not been adequately described. We have focused on sca-1+ endothelial cells (SPEC: sca-1+CD31+CD45− cells) and analyzed their localization, growth potential, and the role of these cells in damaged liver. SPECs are localized in the portal area and comprise approximately 20–30% of CD31+CD45− cells. These cells have higher growth potential than sca-1− endothelial cells and grow aggressively when the liver is severely damaged on the lateral side of the oval cells. In an *in vivo* study we show that when the liver is severely damaged in the presence of a VEGF (vascular endothelial growth factor)-inhibitor, the frequency of SPECs decreased and the recovery of liver volume was also delayed. These results strongly suggest that SPECs play important roles in the recovery of severely damaged liver.

Keywords: Sca-1; Endothelial cells; Liver regeneration; Oval cells; VEGF; Portal area; Mouse; Cytokeratin; CD31; Acute liver disease

The liver exhibits a great regenerative potential after acute or chronic liver damage. When liver damage occurs more rapidly than regeneration, liver failure will occur and thus management of liver function will be necessary in order to prolong life. Researches focused on hepatocytes and hepatic stem/progenitor cells have been progressing rapidly. In addition, Kupffer cells, stellate cells and sinusoidal endothelial cells are known to be important cells for liver regeneration [1,2] and HGF (hepatocytes growth factor) [3], EGF (epidermal growth factor) [4], insulin [4], IL-6 (interleukin) [5], and TNF-α (tumor necrosis factor) [6,7], have been shown to accelerate the regeneration [8]. Endothelial cells in the portal area during liver damage however, have not been aggressively investigated. This investigation may contribute to the efficient angiogenesis and liver regeneration.

Previously, we have reported a serum-free culture system for the expansion of fetal and postnatal hepatic stem/progenitor cells [9,10]. In these studies we found that although sca-1 expressing hepatic progenitor cells were present in our culture, the main population of sca-1 expressing cells in the liver is the endothelial cells. Sca-1 is known as a stem cell marker for hematopoietic cells [11], mesenchymal cells [12], heart [13], mammary gland

☆ Financial support: This work was supported by a Grant-in-Aid for Creative Scientific Research (13GS0009), and a Grant-in-Aid for Scientific Research (B) (15039219) from the Ministry of Education, Science, Technology, Sports and Culture of Japan. This work was also supported by a Grant from Viral Hepatitis Research Foundation of Japan.
* Corresponding author. Fax: +81 75 752 2361.
E-mail address: tnakaha@kuhp.kyoto-u.ac.jp (T. Nakahata).

0006-291X/$ - see front matter © 2007 Published by Elsevier Inc.
doi:10.1016/j.bbrc.2007.10.150

[14], testis [15], and prostate gland [16]; however, few reports describe the function of sca-1. A study using sca-1 null mice revealed that the hematopoietic stem cells in these mice are defective in function, and their progenitor cells exhibit abnormal differentiation [17–20]. Furthermore, sca-1 null mice have a higher risk of osteoporosis than control mice [12]. These results revealed that the function of sca-1 is important for stem cell and progenitor cell self-renewal or differentiation. In this study, we have investigated sca-1+ cells in the liver, with a particular focus on the predominant population of sca-1+ endothelial cells. Matsumoto et al. have previously reported that in the developing liver, flk-1+ immature endothelial cells that do not form blood vessels are important for the extensive expansion of fetal hepatic cells [21]. We therefore predicted that sca-1+ endothelial cells are immature and necessary for rapid liver regeneration.

Reports studying sca-1+ endothelial cells are very rare and to our knowledge only two groups have described these cells. Cherqui et al. showed that sca-1+ endothelial cells have a highly angiogenic capacity and are present in the fetal liver [22]; however, the function and relationship of these cells to liver development remains unclear. In a second study, Luna et al. reported that sca-1+ endothelial cells are present in the liver as sca-1+CD31+ cells [23]. We now know however, that there are two populations of sca-1+CD31+ cells; sca-1+CD31+CD45+ cells and sca-1+CD31+CD45− cells, although the localization and frequency of these cells remains to be determined.

In this study we have determined that sca-1+ endothelial cells are indeed present in the liver. We speculated that sca-1+ endothelial cells are immature and have an important role in the remodeling of damaged livers. We examined the frequency and distribution of sca-1+ endothelial cells in the normal and damaged liver, as well as their growth potential and their role in liver regeneration, especially from oval cells to hepatocytes.

Materials and methods

Mice and liver dissociation. C57BL/6 mice (4-, 8-, 12-weeks old: 5 mice per each group) were obtained from SLC (Hamamatsu, Japan). Mice were maintained according to the Animal Protection Guidelines of Kyoto University. The livers from these mice were dissociated using a modified two step collagenase method. The mice were initially anesthetized with diethylether. A celiotomy was performed and a 24G indwelling needle was inserted into the abdominal inferior vena cava. After the insertion, thoracotomy, chest inferior vena cava ligation, and portal vein dissection were performed as swiftly as possible. Then, 30 ml Liver perfusion Medium (Gibco BRL, Grand Island, NY) and 50 ml Liver Digest Medium (Gibco) at 37 °C were perfused for 3–4 min each. The perfused livers were placed into 6 cm-diameter culture dishes and incubated at 37 °C for 8 min before they were dissociated in the DMEM/F12 (1:1; Sigma, St. Louis, MO) with 10% fetal bovine serum (Sigma), 10 mM HEPES (Nakalai Tesque, Inc. Kyoto, Japan), and antibiotics. Dissociated cells were filtered once with a 70 μm mesh and twice with a 40 μm mesh, and single cells were obtained. The single cell suspension was separated into 15 ml conical tubes and centrifuged at 250 rpm for 1 min. The supernatant was collected and centrifuged at 500 rpm for 1 min before the supernatant was again centrifuged at 500 rpm for 1 min. Finally, the supernatant was centrifuged at 1000 rpm for 3 min and the collected cells were cultured or analyzed.

Acute liver damaged mouse model. We used 4-weeks old mice to generate a mouse model with acute liver damaged. Liver damage was induced by the intraperitoneal injection of 12 μl (0.5 mg/ml) anti-Fas antibody (BD PharMingen, San Diego, CA) dissolved in 200 μl PBS (Phosphate Buffered Saline) three times (at days 1, 4, 7: 5 mice per each group). Livers were analyzed by flow cytometry or immunohistochemistry 2-, 4-, and 6-days after the last injection of anti-Fas antibody.

Flow cytometry. Dissociated normal and damaged liver cells were used to analyze sca-1+ cells in the liver. The resulting cells were incubated with anti-mouse CD16/32 antibodies (PharMingen) for 15 min on ice to block non-specific binding and then incubated with fluorescein isothiocyanate (FITC)-conjugated sca-1 antibodies, phycoerythrin (PE)-conjugated CD31, or allophycocyanin (APC)-conjugated CD45 antibodies (PharMingen) for 30 min on ice. FITC-conjugated rat IgG2a antibodies, PE-conjugated rat IgG2a antibodies or APC-conjugated rat IgG2b antibodies (PharMingen) served as isotype controls. After washing, the cells were analyzed or sorted using FACSCalibur or FACSVantage.

Immunochemical staining. Immunocytochemistry; cells were washed in PBS, fixed with methanol (Wako, Osaka, Japan) at −20 °C for 10 min, incubated with primary antibody overnight at 4 °C and then the appropriate secondary antibody for 30 min at room temperature. Antibodies were diluted to their optimal concentrations in PBS containing 0.1% saponin. The primary antibody used was rat anti-CD31 (PharMingen) and the secondary antibody was Cy3-conjugated donkey anti-rat IgG (Jackson ImmunoResearch Laboratories, Inc., West Grove, PA). Immunohistochemistry; livers were collected, fixed in 10% formalin, processed using a standard protocol, and embedded in paraffin blocks. 4 micrometer sections were cut and placed on silane-coated slides. After removing the paraffin, antigen retrieval was performed using proteinase K (Dako, Kyoto, Japan) for 3 min. Endogenous peroxidase activity was blocked with 3% hydrogen peroxide in methanol (Wako, Osaka, Japan) for 10 min at room temperature, and sections were incubated with primary antibodies diluted with PBS containing 0.1% saponin. The primary antibodies used were rat anti-mouse sca-1 (Pharmingen), and rabbit anti-cow cytokeratin (CK; Dako, Z0622), which detects bile ducts and oval cells. For DAB (3,3′-diaminobenzidine tetrahydrochloride) staining, slides were then stained using Histofine Simple Stain Max-PO (Nichirei Bioscience Inc, Tokyo, Japan) and DAB Substrate Kit (Vector Laboratories, Burlingame, CA) for sca-1, and the Vectastain. ABC Kit and DAB Substrate Kit (Vector Laboratories) for anti-cow CK. For the immunofluorescence double staining of sca-1 and CK, FITC-conjugated donkey anti-rat IgG and Cy3-conjugated donkey anti-rabbit IgG were used as the secondary antibodies. Normal IgG of the species from which the primary antibodies had been obtained served as primary antibodies in the negative controls. Nuclei were stained using Mayer's hematoxylin solution (Wako).

Endothelial cell culture. We employed two methods to culture endothelial cells using the CS-C Complete Medium Kit (Cell Systems, Kirkland, WA). The medium was changed every 3 days. In the first method, 2×10^5 dissociated cells from normal or damaged livers were plated on 6 cm-diameter collagen coated dishes for 6 days. At day 6, cultured cells were stained with anti-CD31 and the area of the dish covered by CD31+ cells was determined in order to analyze the growth potential of SPECs and SNECs. The second method used dissociated cells that were sorted using FACS Vantage. 15,000 cells from normal or damaged livers were plated on 6 cm collagen coated dishes. Five days after plating, the number of cell clusters that contained more than 4 cells was counted in order to analyze the growth potential of SPECs and SNECs.

Functional analysis of SPECs. To analyze the function of SPECs, the mice with anti-Fas-induced liver damage were separated by two groups (5 mice per each group), and were treated with or without VEGF-inhibitor. VEGF inhibitor (CBO-P11, Sigma, 0.2 mg/mice) was dissolved in DMSO (dimethylsulfoxide), and used to fill Osmotic Pumps (DURECT Corp., Cupertino, CA) that were subsequently implanted intraperitoneally into the mice. Osmotic Pumps released the VEGF-inhibitor continuously throughout the experiments. To analyze the effect of the VEGF-inhibitor on SPECs and liver regeneration, the frequency of sca-1+ endothelial cells

in the CD31+CD45− cells as well as the liver volume as the percentage of the total body weight was analyzed 2-, 4-days after the last injection of anti-Fas antibody.

Statistical analysis. The data are presented as means ± SD. The Student's *t* test was used to determine the statistical significance of observed differences.

Results

SPECs reside in the portal area

In order to determine which cells expressed sca-1 in the liver, we analyzed dissociated liver cells by flow cytometry. After liver dissociation, concentrated non-parenchymal cells were analyzed by flow cytometry. A fraction of small cells were gated to exclude parenchymal cells and dead cells (Fig. 1A). To determine whether the frequency of sca-1-expressing cells varied with age we analyzed liver cells from 4weeks, 8 weeks, and 12 weeks old mice (5 mice per each group). We identified four populations of sca-1+ cells in non-parenchymal population; (1) sca-1+CD31+CD45− cells, (2) sca-1+CD31+CD45+ cells, (3) sca-1+CD31−CD45+ cells, and (4) sca-1+CD31−CD45− cells (Fig. 1B–E). CD45 is a hematopoietic marker, therefore populations (2) and (3) were hematopoietic cells. The main population of sca-1+ cells was sca-1+CD31+CD45−

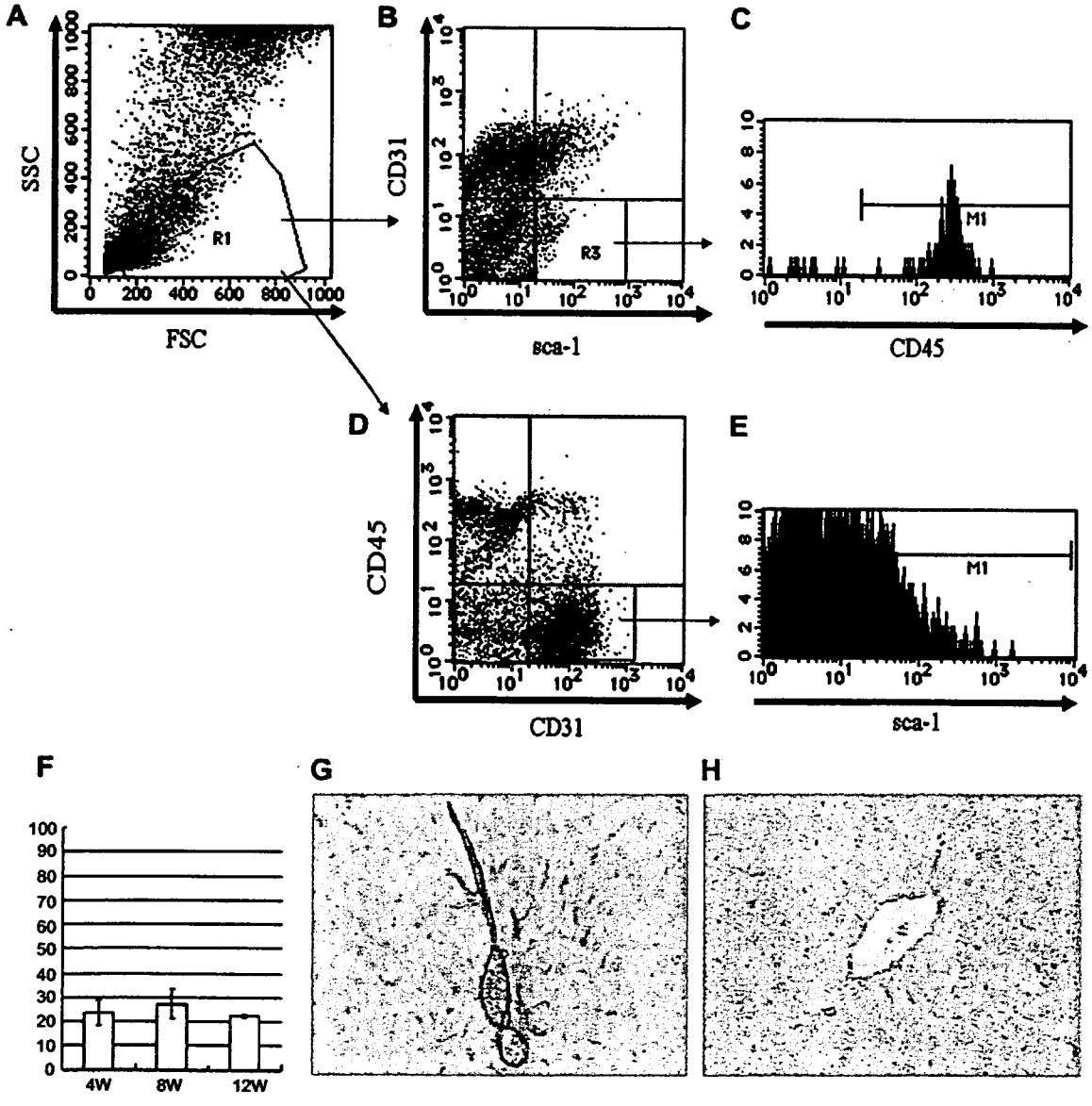

Fig. 1. Flow cytometric analysis and immunocytochemistry of SPECs in the normal liver. (A–F) Flow cytometric analysis of the dissociated normal liver cells. (A) Dissociated cells were gated according to forward scatter (FCS) and side scatter (SSC). Parenchymal cells and dead cells were excluded as much as possible. (B–E) Most of the sca-1+CD31− cells were CD45+ hematopoietic cells. Of the CD31+CD45− cells, approximately 20–30% were sca-1+. (F) The frequency of SPECs did not change with age. (G,H) Immunocytochemistric analysis of normal liver. Sca-1+ endothelial cells reside in the portal area (G) and not in the central vein (H).

endothelial cells (population 1: Fig. 1E). The frequency of sca-1+CD31+CD45− within the CD31+CD45− cell population was approximately 20–30% and the frequency did not change with the age of the mice (Fig. 1F). Surprisingly, immunohistochemistry for sca-1 revealed that sca-1+ cells reside in or around the portal area but not around the central vein (Fig. 1G and H). We named the sca-1+CD31+CD45− cells SPECs (sca-1 positive endothelial cells) and sca-1-CD31+CD45− cells SNECs (sca-1 negative endothelial cells).

SPECs expanded along the lateral side of oval cells during acute liver damage

SPECs were localized in the portal area of the liver, therefore we analyzed the frequency of SPECs during acute liver damage. In order to induce severe liver damage, 4-weeks old mice were injected three times with anti-Fas (Jo-2) antibody (days 1, 4, and 7). A large number of oval cells were detected by immunohistochemistry using an anti-cytokeratin antibody in the liver samples from treated mice (Fig. 2D–G). 2-, 4-, and 6-days after the last anti-Fas antibody injection, we analyzed the frequency of SPECs in the CD31+CD45− cells. On day 2, the frequency of SPECs in the CD31+CD45− cells had increased by approximately 60%; this number then gradually decreased with time (Fig. 2A–C). These results indicated that SPECs play important roles in the recovery from acute liver damage. Immunocytochemical analysis of the damaged livers revealed that SPECs were localized in or around the portal area and not around the central vein (Fig. 2A–C). The relationship between SPECs and oval cells was analyzed by double staining with sca-1 and anti-CK (oval cells). Interestingly, this staining revealed that sca-1+ endothelial cells extended along the lateral side of oval cells (Fig. 2G). These results strongly suggest that SPECs are necessary for the expansion or differentiation of oval cells.

SPECs exhibit higher growth potential comparing with SNECs

Two experiments were performed to compare the growth potential of SPECs and SNECs. Firstly, crude endothelial cells were obtained from normal livers and from livers damaged using an anti-Fas antibody. The frequency of SPECs in crude endothelial cells prepared from damaged livers was more than twofold higher than those obtained from normal livers. Six days after the culture started, the area of endothelial cells was analyzed by immunocytochemistry using an anti-CD31 antibody. While crude endothelial cells from normal livers formed small sheets of CD31+ endothelial cells, crude endothelial cells from damaged livers formed more than fivefold larger sheets of endothelial cells than those from normal livers (Fig. 3A–D). In the second experiment, we cultured 15,000 sorted SPECs and SNECs for 6 days on 6 cm collagen-coated dishes, and subsequently counted the cell groups that consisted of more than 4 cells. It is difficult to maintain and grow sorted endothelial cells; however counted cell groups of SPECs were approximately fivefold higher than those of SNECs (Fig. 3E–G). These two experiments revealed that SPECs have higher growth potential than SNECs.

VEGF-inhibitor decreased the frequency of SPECs and also delayed the recovery from acute liver damage

As SPECs have a higher growth potential than SNECs and grow along the lateral side of oval cells, we speculated that SPECs have an important role in liver regeneration in response to acute liver damage. To test this hypothesis, mice with anti-Fas antibody-induced acute liver damage were separated into two groups. We implanted an osmotic pump containing either the VEGF-inhibitor (group 1: dissolved in DMSO) or no VEGF-inhibitor (group 2: DMSO only as a vehicle control) into the peritoneum of each mouse. Osmotic Pumps released VEGF-inhibitor (CBO-P11, 0.2 mg/mice) or DMSO continuously throughout the experiments. At 2 or 4 days after the last anti-Fas antibody injection, we analyzed the frequency of SPECs in the CD31+CD45− cells and the liver weight as a percentage of the total body weight. At day 4, the frequency of SPECs and the liver weight was lower in group 1 than group 2 (Fig. 4A and B). Continuous injection of VEGF-inhibitor strongly inhibited the growth of SPECs and furthermore delayed the liver regeneration. These results strongly suggest that SPECs play an important role in the early recovery from acute liver damage.

Discussion

The liver exhibits the potential to regenerate in response to acute and chronic damage [1]. For example, after partial hepatectomy preexisting hepatocytes continued to divide and thus contributed to the recovery of the liver volume [1]. During severe acute liver injury, this system cannot maintain liver function. In these cases, it is commonly believed that oval cells contribute to the recovery of hepatocytes. Most of the cases of acute liver damage can be overcome by bed rest. However, during fulminant hepatic failure, a therapeutic margin still exists even after combined modality therapy. In these cases, liver transplantation is often the only the way to rescue the patient. The degree of liver damage may be the important deciding factor; however, we think that appropriate liver regeneration from oval cells to hepatocytes could have the potential to rescue some patients from fulminant hepatic failure.

We found that the population of sca-1+ cells in the liver was predominantly composed of endothelial cells (SPECs), and these were the focus of our study. Endothelial cells in the liver can be divided into 2 groups; SPECs (sca-1+ endothelial cells) and SNECs (sca-1− endothelial cells). SPECs have some intriguing aspects, the most intriguing of which is their localization. In this study we found that

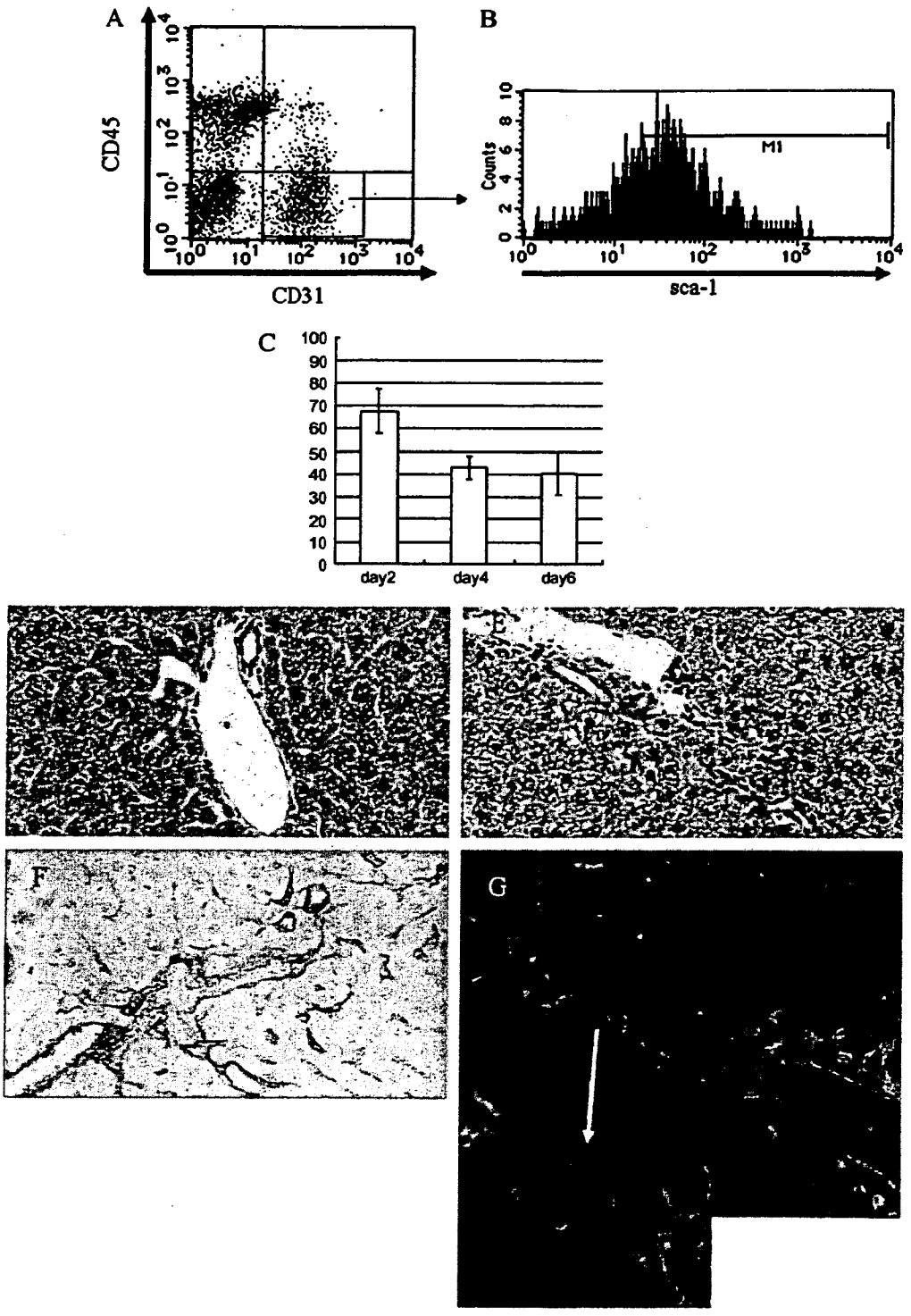

Fig. 2. Flow cytometric analysis and immunocytochemistry of SPECs in the damaged liver. (A–C) Flow cytometric analysis of the dissociated damaged liver cells. (B,C) after the damage, the frequency of sca-1+ cells within the CD31+CD45− cell population increased rapidly and then gradually decreased(B,C; at day 2 after the last anti-Fas antibody injection). Hematoxylin-eosin staining of normal (D) and damaged livers (E) at day 4 after the last anti-Fas injection. Immunocytochemistry of sca-1+ cells and oval cells revealed that SPECs grow at the lateral side of oval cells (F,G; green: oval cells, red: SPECs). (For interpretation of the references to color in this figure legend, the reader is referred to the web version of this paper.)

the localization of SPECs was limited to the vicinity of the portal area, not in the vicinity of the central vein. Interestingly, their frequency was elevated in response to acute liver damage. Furthermore, when the liver was damaged severely, the localization of SPECs extended along the lateral side of oval cells. In addition, continuous administra-

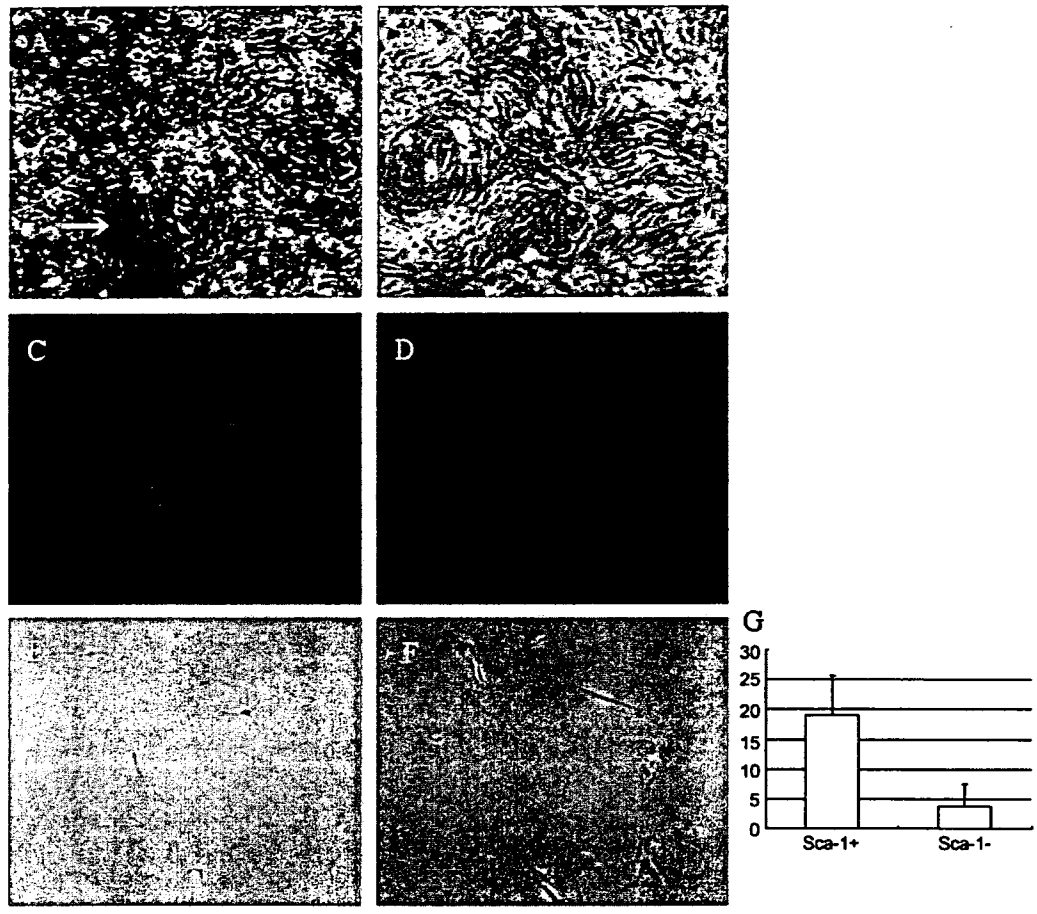

Fig. 3. Growth potential of SPECs and SNECs. (A–G) crude cell culture and sorted cell culture. (A–D) crude dissociated cell culture from normal and damaged livers revealed that the area of endothelial cells from damaged liver cells (A,B; spindle shaped cells indicated by white arrow: endothelial cells, C; red: CD31+ endothelial cells) was wider than those from normal livers (B, D). (E–G) Cell culture of sorted SNECs (E) and SPECs (F) revealed that SPECs have a greater growth potential than SNECs. (For interpretation of the references to color in this figure legend, the reader is referred to the web version of this paper.)

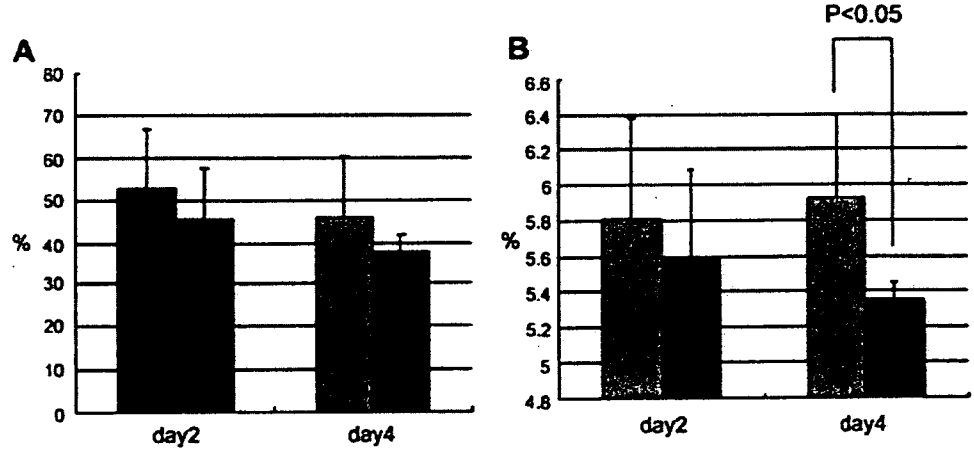

Fig. 4. Role of SPECs in *in vivo* model. (A,B) Analysis of SPECs in an *in vivo* model. (A) The frequency of SPECs from damaged livers treated with no VEGF-inhibitor (A, red) was higher than that in damaged livers treated with VEGF inhibitor (A, blue). In contrast, liver weight per body weight (%) of damaged mice treated with no VEGF inhibitor (B, red) was higher than that in damaged mice treated with VEGF-inhibitor. (For interpretation of the references to color in this figure legend, the reader is referred to the web version of this paper.)

tion of a VEGF-inhibitor to mice with severe liver damage decreased the frequency of SPECs and prolonged the recovery of the liver size. Indeed, Namisaki et al. previously reported that VEGF had a salvage effect on chemically induced acute severe liver injury in rats [24], and this result supports our conclusions. SPECs function to form a passage leading from bile duct to hepatocytes, and may also directly or indirectly influence the growth and differentiation of oval cells. We believe that sca-1+ endothelial cells play an important role in the remodeling of damaged liver. Sca-1 is a marker unique to mice and thus cannot be used in human studies. In the future we believe that a common system will allow the analysis of SPECs in mice and in humans, and will thus help to elucidate the role of oval cells in human disease. In addition, our study implies that effective angiogenesis therapy may improve the ability of the liver to regenerate, and hence improve the therapeutic outcome for patients.

References

[1] N. Fausto, J.S. Campbell, K.J. Riehle, Liver regeneration, Hepatology 43 (2006) S45–S53.

[2] R. Malik, C. Selden, H. Hodgson, The role of non-parenchymal cells in liver growth, Semin. Cell. Dev. Biol. 13 (2002) 425–431.

[3] K. Matsumoto, T. Nakamura, Hepatocyte growth factor: molecular structure, roles in liver regeneration, and other biological functions, Crit. Rev. Oncog. 3 (1992) 27–54.

[4] H.S. Lai, Y.C. Chung, W.J. Chen, K.M. Chen, Rat liver regeneration after partial hepatectomy: effects of insulin, glucagon and epidermal growth factor, J. Formos. Med. Assoc. 91 (1992) 685–690.

[5] A. Blindenbacher, X. Wang, I. Langer, R. Savino, L. Terracciano, M.H. Heim, Interleukin 6 is important for survival after partial hepatectomy in mice, Hepatology 38 (2003) 674–682.

[6] H. Hayashi, M. Nagaki, M. Imose, Y. Osawa, K. Kimura, S. Takai, M. Imao, T. Naiki, T. Kato, H. Moriwaki, Normal liver regeneration and liver cell apoptosis after partial hepatectomy in tumor necrosis factor-alpha-deficient mice, Liver Int. 25 (2005) 162–170.

[7] P.A. Gruppuso, J.E. Mead, N. Fausto, Transforming growth factor receptors in liver regeneration following partial hepatectomy in the rat, Cancer Res. 50 (1990) 1464–1469.

[8] R. Taub, Liver regeneration: from myth to mechanism, Nat. Rev. Mol. Cell Biol. 5 (2004) 836–847.

[9] A. Tsuchiya, T. Heike, S. Baba, H. Fujino, K. Umeda, Y. Matsuda, M. Nomoto, T. Ichida, Y. Aoyagi, T. Nakahata, Long-term culture of postnatal mouse hepatic stem/progenitor cells and their relative developmental hierarchy, Stem Cells (2007).

[10] A. Tsuchiya, T. Heike, H. Fujino, M. Shiota, K. Umeda, M. Yoshimoto, Y. Matsuda, T. Ichida, Y. Aoyagi, T. Nakahata, Long-term extensive expansion of mouse hepatic stem/progenitor cells in a novel serum-free culture system, Gastroenterology 128 (2005) 2089–2104.

[11] S. Okada, H. Nakauchi, K. Nagayoshi, S. Nishikawa, Y. Miura, T. Suda, In vivo and in vitro stem cell function of c-kit- and Sca-1-positive murine hematopoietic cells, Blood 80 (1992) 3044–3050.

[12] M. Bonyadi, S.D. Waldman, D. Liu, J.E. Aubin, M.D. Grynpas, W.L. Stanford, Mesenchymal progenitor self-renewal deficiency leads to age-dependent osteoporosis in Sca-1/Ly-6A null mice, Proc. Natl. Acad. Sci. USA 100 (2003) 5840–5845.

[13] K. Matsuura, T. Nagai, N. Nishigaki, T. Oyama, J. Nishi, H. Wada, M. Sano, H. Toko, H. Akazawa, T. Sato, H. Nakaya, H. Kasanuki, I. Komuro, Adult cardiac Sca-1-positive cells differentiate into beating cardiomyocytes, J. Biol. Chem. 279 (2004) 11384–11391.

[14] B.E. Welm, S.B. Tepera, T. Venezia, T.A. Graubert, J.M. Rosen, M.A. Goodell, Sca-1(pos) cells in the mouse mammary gland represent an enriched progenitor cell population, Dev. Biol. 245 (2002) 42–56.

[15] M.P. van Bragt, N. Ciliberti, W.L. Stanford, D.G. de Rooij, A.M. van Pelt, LY6A/E (SCA-1) expression in the mouse testis, Biol. Reprod. 73 (2005) 634–638.

[16] L. Xin, D.A. Lawson, O.N. Witte, The Sca-1 cell surface marker enriches for a prostate-regenerating cell subpopulation that can initiate prostate tumorigenesis, Proc. Natl. Acad. Sci. USA 102 (2005) 6942–6947.

[17] S.B. Bradfute, T.A. Graubert, M.A. Goodell, Roles of Sca-1 in hematopoietic stem/progenitor cell function, Exp. Hematol. 33 (2005) 836–843.

[18] C.Y. Ito, C.Y. Li, A. Bernstein, J.E. Dick, W.L. Stanford, Hematopoietic stem cell and progenitor defects in Sca-1/Ly-6A-null mice, Blood 101 (2003) 517–523.

[19] W.L. Stanford, S. Haque, R. Alexander, X. Liu, A.M. Latour, H.R. Snodgrass, B.H. Koller, P.M. Flood, Altered proliferative response by T lymphocytes of Ly-6A (Sca-1) null mice, J. Exp. Med. 186 (1997) 705–717.

[20] Z.X. Zhang, W.L. Stanford, L. Zhang, Ly-6A is critical for the function of double negative regulatory T cells, Eur. J. Immunol. 32 (2002) 1584–1592.

[21] K. Matsumoto, H. Yoshitomi, J. Rossant, K.S. Zaret, Liver organogenesis promoted by endothelial cells prior to vascular function, Science 294 (2001) 559–563.

[22] S. Cherqui, S.M. Kurian, O. Schussler, J.A. Hewel, J.R. Yates 3rd, D.R. Salomon, Isolation and angiogenesis by endothelial progenitors in the fetal liver, Stem Cells 24 (2006) 44–54.

[23] G. Luna, J. Paez, J.E. Cardier, Expression of the hematopoietic stem cell antigen Sca-1 (LY-6A/E) in liver sinusoidal endothelial cells: possible function of Sca-1 in endothelial cells, Stem Cells Dev. 13 (2004) 528–535.

[24] T. Namisaki, H. Yoshiji, H. Kojima, J. Yoshii, Y. Ikenaka, R. Noguchi, S. Sakurai, K. Yanase, M. Kitade, M. Yamazaki, K. Asada, M. Uemura, M. Nakamura, H. Fukui, Salvage effect of the vascular endothelial growth factor on chemically induced acute severe liver injury in rats, J. Hepatol. 44 (2006) 568–575.

Pathology International 2007; **57**: 82–90 doi:10.1111/j.1440-1827.2006.02061.x

Original Article

Downregulated P1 promoter-driven hepatocyte nuclear factor-4α expression in human colorectal carcinoma is a new prognostic factor against liver metastasis

Tomoko Oshima,[1,2] Takashi Kawasaki,[1] Riuko Ohashi,[1] Go Hasegawa,[1] Shuying Jiang,[1,3] Hajime Umezu,[1] Yutaka Aoyagi,[2] Hiroko Iwanari,[3] Toshiya Tanaka,[4] Takao Hamakubo,[4] Tatsuhiko Kodama[4] and Makoto Naito[1]

Divisions of [1]Cellular and Molecular Pathology and [2]Gastroenterology and Hepatology, Niigata University Graduate School of Medical and Dental Sciences, Niigata, [3]Perseus Proteomics, Tokyo and [4]Laboratory for Systems Biology and Medicine, Research Center for Advanced Science and Technology, University of Tokyo, Tokyo, Japan

Liver metastases are the most critical prognostic factors for patients with colorectal carcinomas (CRC). It has been reported that the dysregulation of hepatocyte nuclear factor-4α (HNF4α) expression is linked to the development of CRC, gastric cancer and hepatocellular carcinoma. The purpose of the present paper was to examine the P1 and P2 promoter-driven HNF4α (P1 and P2) expression in surgically resected CRC. Immunohistochemically, P1, P2, MUC1 and CD10 expression were evaluated in 63 cases of primary CRC. Positive staining with P1, P2, MUC1 and CD10 antibodies were observed in 37 (59%), 63 (100%), 42 (67%) and 27 (43%) cases, respectively. Loss or decreased P1 expression was observed with respect to the depth of the tumor invasion. The frequency of P1-positive expression in Dukes' C and D tumors was significantly lower than that in Dukes' A and B tumors. There was a relationship between the loss of P1 expression and metachronous liver metastases, and the survival rate of the P1-negative patients without liver metastasis at the time of the primary CRC resection tended to be worse than that of the P1-positive patients. These findings suggest that downregulation of P1 expression is involved in tumor metastasis and a worse prognosis.

Key words: colorectal carcinoma, hepatocyte nuclear factor-4α (HNF4α), liver metastasis, P1 promoter

Age-adjusted death rates for malignant neoplasm in Japan in 2003 show that the number of patients with colorectal carcinomas (CRC) increases year by year, and CRC are the fourth most common cancer in male and the first in female subjects.[1] Surgical therapy is the first choice, and the 5 year survival rate for curative post-surgical patients is good at approximately 80%, but the patients with liver metastases have a poor outcome. It has been reported that liver metastases are found in approximately 10–30% of patients at the time of the primary CRC resection,[2,3] and metachronous liver metastases are also found in 5–6% of patients.[3] The early detection of liver metastasis is important for improving patient survival.

MUC1 or CD10 expression in CRC have been reported to be related to tumor growth pattern, aggressiveness and prognosis. MUC1 expression is upregulated not only in colorectal cancer, but also in breast cancer and cholangiocarcinoma of the liver.[4–6] The upregulation of MUC1 in CRC is distinctly related to tumor invasion, lymph node metastasis and Dukes' classification. MUC1 is also one of the predictive factors for liver metastasis.[4,7,8] CD10 is normally expressed in the brush border of the small intestine, and CD10 expression in CRC is related to venous invasion and liver metastasis.[9,10]

Hepatocyte nuclear factor-4α (HNF4α) is an orphan member of the nuclear receptor superfamily involved in various processes that could influence endoderm development, glucose and lipid metabolism,[11–13] To date, there are at least nine different splicing variants (HNF4α1–α9) in mammals.[14] Exon 1A corresponds to the first exon originally described for the HNF4α1 promoter (P1 promoter), which can generate six different isoforms (HNF4α1–α6). The P2 promoter-driven HNF4α7–α9 is characterized by an alternative first exon 1D.[15] We have reported that the P1 promoter-driven HNF4α is expressed in hepatocytes of liver cells, proximal tubular epithelial cells of the kidney and mucosal epithelial cells of the small intestine and colon.[14] Likewise,

Correspondence: Makoto Naito, MD, PhD, Division of Cellular and Molecular Pathology, Niigata University Graduate School of Medical and Dental Sciences, Asahimachi-dori 1-757, Niigata 951-8510, Japan. Email: mnaito@med.niigata-u.ac.jp

Received 11 September 2006. Accepted for publication 3 October 2006.

changes in the HNF4α expression have been implicated in the pathogenesis of renal cell carcinoma, hepatocellular carcinoma and CRC. HNF4α was reduced in human renal cell carcinoma compared with the normal renal tissue.[16] The loss of HNF4α expression in the model mouse caused the change from a well-differentiated slow-growing transplantable hepatocellular carcinoma to a highly invasive fast-growing dedifferentiated variant.[17] P1-promoter-driven HNF4α (P1) appears to decrease in hepatocellular carcinoma and CRC.[15] These reports suggest that the loss of HNF4α expression may be related to tumorigenesis, aggressiveness and metastases.

We have examined the expression of HNF4α (P1 and P2) in CRC and its liver metastases, compared with those of MUC1 and CD10. While apparent relationships were not observed between the expressions of P2, MUC1 and CD10 and liver metastases, we have found a significant difference between the loss of P1 expression and metachronous liver metastases. The survival rate in P1-negative cases without liver metastasis at the time of the primary CRC resection tended to be worse than that in P1-positive cases.

MATERIALS AND METHODS

Patients

Sixty-three cases of primary CRC were randomly selected from patients undergoing tumor resection at the Division of Surgery, Niigata University Graduate School of Medical and Dental Science from 1998 to 2004. Non-neoplastic colon tissues were also obtained from those patients. Sample processing and handling were carried out following the guidelines of Niigata University Medical and Dental Hospital for Research, with patient consent. Thirty-four were male and the remaining 29 were female (Table 1). The mean age was 65 years with a range of 34–85 years. The histological classification was based on the Japanese Classification of Colorectal Carcinoma. There were 63 adenocarcinomas, including 37 well-differentiated adenocarcinomas (58.7%), 24 moderately differentiated adenocarcinomas (38.1%), and two mucinous carcinomas (3.2%). There were no poorly differentiated adenocarcinomas. The tumor location was the cecum in five (7.9%), ascending colon in 12 (19.0%), transverse colon in two (3.2%), descending colon in two (3.2%), sigmoid colon in 12 (19.0%) and rectum in 30 patients (47.6%). The depth of tumor invasion was sm (pT1) in 0 (0%), mp (pT2) in seven (11.1%), ss (pT3) in 39 (61.9%) and se or si (pT4) in 17 (27.0%). Dukes' classification was A in two (3.2%), B in 13 (20.6%), C in 13 (20.6%) and D in 35 (55.6%). The liver metastases were observed in 35 patients. Of the 35 CRC with liver metastases, 23 were synchronous metastases (36.5%), and the other 12 were metachronous metastases (19.0%).

Table 1 Clinicopathological features of the CRC patients

	No. patients ($n = 63$) n (%)
Age	
(years)	34–85
(mean)	65
Gender	
Male	34 (54.0)
Female	29 (46.0)
Histological type	
Well	37 (58.7)
Mod	24 (38.1)
Muc	2 (3.2)
Tumor location	
Cecum	5 (7.9)
Ascending	12 (19.0)
Transverse	2 (3.2)
Descending	2 (3.2)
Sigmoid	12 (19.0)
Rectum	30 (47.6)
Depth of the invasion	
Tis/T1	0 (0)
T2	7 (11.1)
T3	39 (61.9)
T4	17 (27.0)
Dukes' classification	
A	2 (3.2)
B	13 (20.6)
C	13 (20.6)
D	35 (55.6)
Liver metastasis	
Synchronous	23 (36.5)
Metachronous	12 (19.0)

CRC, colorectal carcinoma; Mod, moderately differentiated adenocarcinoma; Muc, mucinous adenocarcinoma; Well, well-differentiated adenocarcinoma.

Cell culture

Four established human colon carcinomas, Caco2, DLD-1 and HCT116 were kindly gifted from the Advanced Science and Technology Research Center for Cell Resource Center (Tokyo University), and SW480 was obtained from the Biomedical Research Institute of Department of the Aging and Cancer (Tohoku University). Caco2 was derived from well-differentiated adenocarcinoma. DLD-1 was derived from moderately to poorly differentiated adenocarcinoma, and is known as having a rapid downhill clinical course. HCT116 and SW480 were derived from poorly differentiated adenocarcinoma. They were maintained in RPMI 1640 (Sigma-Aldrich, Irvine, UK) supplemented with 10% heat-inactivated fetal bovine serum (JRH Biosiences, Lenexa, KS, USA), 100 units/mL penicillin G sodium and 100 μg/mL streptomycin.

Antibodies

A mouse mAb K9218 (P1) was directed against the A/B region of hHNF4α1 containing the amino acids 3–49 of hHNF4α1.[14] A mouse mAb H6939 (P2) was directed against the amino-terminal region of HNF4α7–α9. A mouse mAb H1415 (P1/P2) recognizes the amino acids 394–461 of hHNF4α2.[15] Each antibody was purchased from Perseus Proteomics (Tokyo, Japan). The mouse mAb Ma695 (MUC1) and 56C6 (CD10) were purchased from Novocastra (Newcastle-upon-Tyne, UK). The mouse mAb JLA20 (Actin) was purchased from Oncogene Sciences (Uniordale, NY, USA). Anti-HNF4α (P1, P2, P1/P2), anti-MUC1 and anti-CD10 antibodies were used for immunohistochemistry at dilutions of 1:100, 1:100 and 1:80, respectively. Anti-HNF4α (P1, P2 and P1/P2) and anti-actin antibodies were used for immunoblotting in dilutions of 1:1000 (P1, P2 and P1/P2) and 1:5000 (actin), respectively.

Immunohistochemistry

Tissue samples were fixed at room temperature in 10% formalin. The samples were sequentially dehydrated with an alcohol series and embedded in paraffin. Four micron-thick sections were cut, deparaffinized in xylene and dehydrated in descending dilutions of ethanol. Specimens were treated by incubating in citrate buffer (P1, P2 and P1/P2, pH 6.5; MUC1 and CD10, pH 6.0) at 121°C for 15 min in an autoclave. After washing in 0.01 mol/L PBS, the endogenous peroxidase activity was blocked by treating for 20 min with 0.3% hydrogen peroxidase in absolute methanol. They were incubated with 10% normal goat serum for 10 min at room temperature and reacted with primary mAb overnight at 4°C. They were incubated for 2 h at room temperature with appropriate secondary antibody (Nichirei, Tokyo, Japan). They were carefully washed three times with PBS, between each step of the procedure. Finally, they were visualized with 0.1 mg/mL 3,3′-diaminobenzidine (DAB) tetrahydrochloride (Dojin Chemical, Kumamoto, Japan). They were counterstained with Mayer's hematoxylin.

Immunoblotting

Immunoblotting was performed as described previously.[18] Briefly, cultured cells were lyzed in a solution containing 150 mmol/L NaCl, 50 mmol/L Tris-HCl (pH 8.0), 5 mmol/L EDTA, 1% Triton X and 1 mmol/L phenylmethylsulfonyl fluoride, 1 mmol/L leupeptin, 1 mmol/L aprotinin for 30 min on ice, and centrifuged at 10 000 *g* at 4°C for 30 min. The extracted protein (20 μg) was resolved by sodium dodecylsulfate–polyacrylamide gel electrophoresis. After electrophoresis, the protein was transferred to PVDF membrane (Amersham, Aylesbury, UK). The blots were pretreated with 5% skim milk overnight, and then incubated with anti-HNF4α (P1, P2 and P1/P2) and anti-actin for 1 h. They were incubated with secondary antimouse IgG horseradish peroxidase-conjugated antibody (Amersham) in a dilution of 1:2000 for 30 min. They were washed three times with PBS, between each step of the procedure. They were visualized with the ECL detection system (Amersham) according to the manufacturer's instructions.

Evaluation and statistical analysis

The extent of P1, CD10 and MUC1 expression was graded semiquantitatively as follows: –, 0% of cells; +/–, positive in <10% of cells; 1+, positive in <50% of cells; 2+, positive in ≥50% of cells; 3+, positive in 100% of cells. Immunoreactivity was estimated as being significantly positive for more than 1+, and significantly negative for less than +/–. The χ^2 test and Fisher's exact test were used to analyze the contingency table. Patient survival was analyzed according to the Kaplan–Meier method. Differences in the survival of the patients in the subgroups were analyzed using the log–rank test. $P < 0.05$ was considered statistically significant.

RESULTS

HNF4α, MUC1 and CD10 expression in primary CRC

All normal colonic mucosa showed nuclear staining with P1, P2 and P1/P2, and no staining with MUC1 and CD10 (Fig. 1). Sixty-three CRC had P1-positive staining in 37 (59%); P2- and P1/P2-positive staining in 63 (100%); MUC1-positive staining in intralumina or partly intracytoplasm in 42 (67%); and CD10-positive staining in intralumina or partly intracytoplasm in 27 (43%), respectively (Fig. 1; Table 2). Additionally, no relationships were found between the expression of HNF4α, MUC1 and CD10 in each case (data not shown).

The frequency of P1-, MUC1- or CD10-positive expression and histological differentiation were not found to be associated with each other (Table 2). P1-positive expression was observed in 86% (6/7) of pT2, 62% (24/39) of pT3 and 41% (7/17) of pT4, and there was a significant difference between pT2 and pT4 tumors ($P < 0.05$; Fig. 2a). MUC1-positive expression was observed in 29% (2/7) of pT2, 72% (28/39) of pT3 and 71% (12/17) of pT4, and there was a significant difference between pT2 and pT3 tumors ($P < 0.05$). There was a tendency toward an association between pT2 and pT4

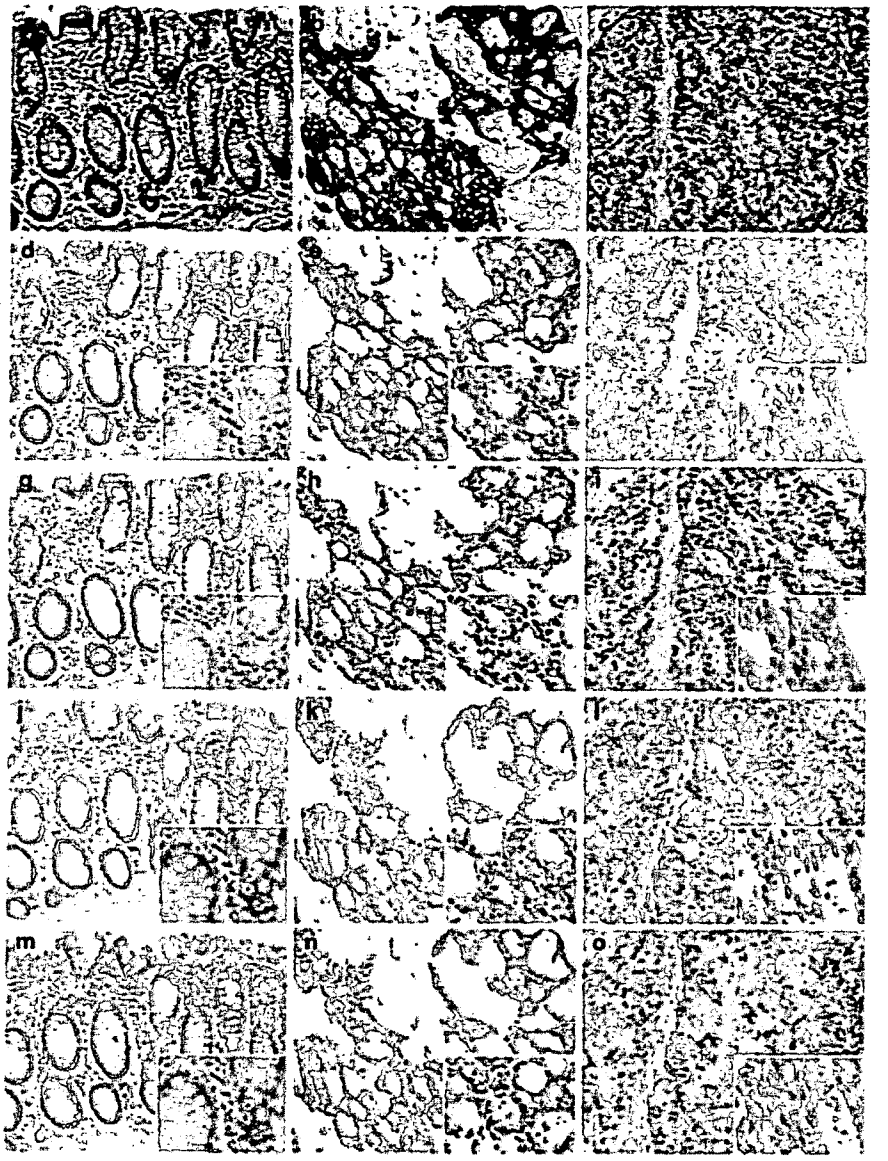

Figure 1 Immunohistochemical expression of each marker in normal colonic mucosa and primary colorectal carcinoma (CRC).Tissue sections of normal colonic mucosa and CRC were stained for P1, P1/P2, MUC1 and CD10. (a) Normal colonic mucosa showed nuclear staining with (d) P1 and (g) P1/P2, and no staining with (j) MUC1 and (m) CD10. (b,c) CRC showed (e) positive or (f) negative P1 staining; (h,l) positive P1/P2 staining; (k,l) positive MUC 1 staining in intralumina or partly intracytoplasm; (n) negative and (o) positive CD10 staining in intralumina and intracytoplasm. Original magnification: ×200; inset, ×400.

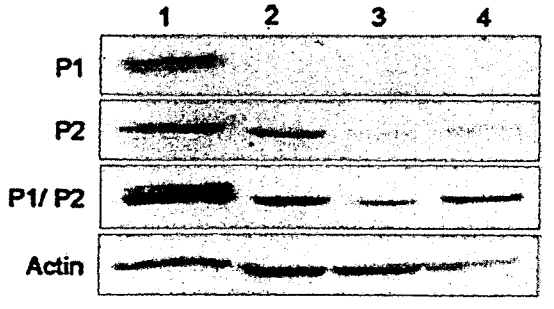

Figure 6 Expression of hepatocyte nuclear factor-4α protein in human colon cancer cell lines. P1 proteins corresponding to 52 kDa were detected in lane 1. P2 and P1/P2 proteins were detected in all lanes. Lane 1, Caco2; lane 2, DLD-1; lane 3, HCT116; lane 4, SW480.

Table 2 Immunohistochemical expression of P1, P2, MUC1, CD10 and histological type of CRC

Histological type	*n*	P1 *n* (%)	P2 *n* (%)	MUC1 *n* (%)	CD10 *n* (%)
Well	37	21 (57)	37 (100)	24 (65)	13 (35)
Mod	24	15 (63)	24 (100)	18 (75)	14 (58)
Muc	2	1 (50)	2 (100)	0 (0)	0 (0)
Total	63	37 (59)	63 (100)	42 (67)	27 (43)

CRC, colorectal carcinoma; Mod, moderately differentiated adenocarcinoma; Muc, mucinous adenocarcinoma; Well, well-differentiated adenocarcinoma.

No difference was observed in the frequency of P1, MUC1 and CD10 positivity with respect to histological differentiation.

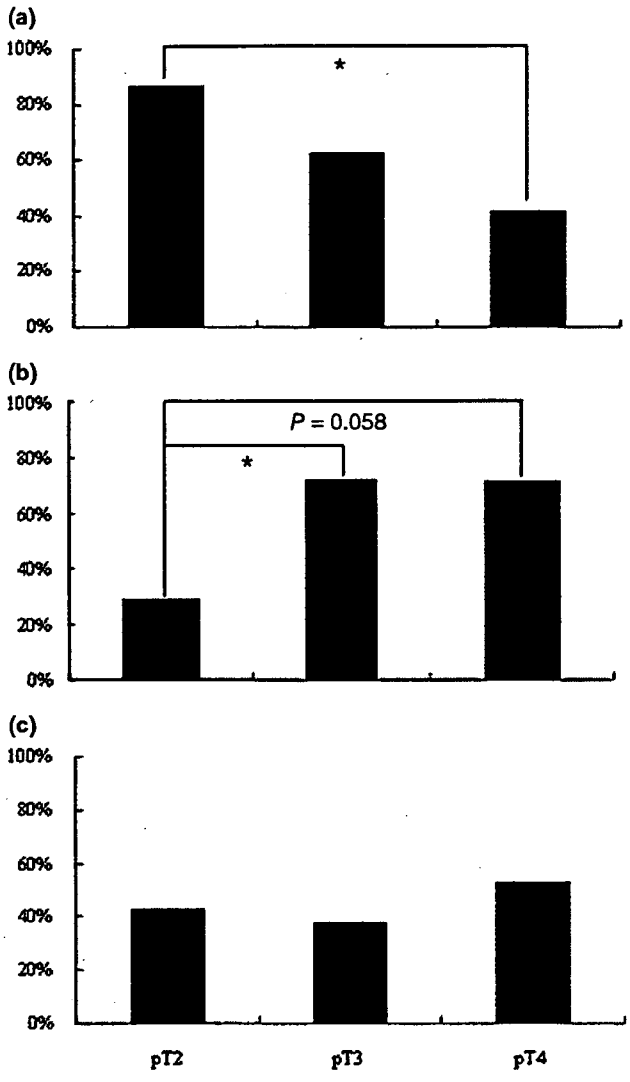

Figure 2 Expression of each marker and depth of cancer invasion. (a) There was a significant difference in the frequency of P1-positive expression between pT2 and pT4 tumors (pT2, 6/7, 86%; pT3, 24/39, 62%; pT4, 7/17, 41%). (b) There was a significant difference in the frequency of MUC1-positive expression between pT2 and pT3 tumors (pT2, 2/7, 29%; pT3, 28/39, 72%; pT4, 12/17, 71%). (c) No significant difference was observed in the frequency of CD10-positive expression (pT2, 3/7, 43%; pT3, 15/39, 38%; pT4, 9/17, 53%). $^*P < 0.05$.

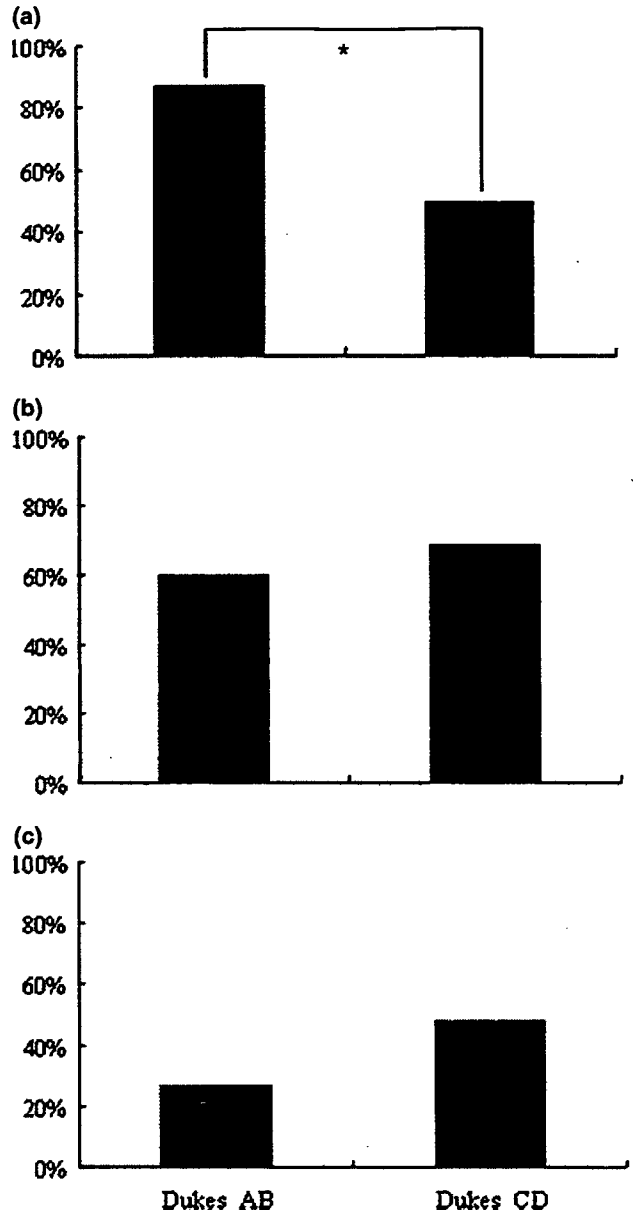

Figure 3 Expression of each marker and Dukes' classification. (a) The frequency of P1-positive expression in Dukes' C and D tumors was significantly lower than that in Dukes' A and B tumors (Dukes' AB, 13/15, 87%; Dukes' CD, 24/48, 50%). (b,c) The frequency of (b) MUC1 or (c) CD10 expression in Dukes' C and D tumors was higher than that in Dukes' A and B tumors, but there were no significant differences, respectively (b, Dukes' AB, 9/15, 60%; Dukes' CD, 33/48, 69%; c, Dukes' AB, 4/15, 27%; Dukes' CD, 23/48, 48%). $^*P < 0.05$.

tumors ($P = 0.058$; Fig. 2b). CD10-positive expression was observed in 43% (3/7) of pT2, 38% (15/39) of pT3 and 53% (9/17) of pT4, and there was no relationship with tumor invasion (Fig. 2c).

P1 positive expression was observed in 100% (2/2) of Dukes' A, 85% (11/13) of Dukes' B, 62% (8/13) of Dukes' C, and 46% (16/35) of Dukes' D. The frequency of P1-positive expression in Dukes' C and D tumors was significantly lower than that in Dukes' A and B tumors ($P < 0.05$; Fig. 3a). In contrast, the frequency of MUC1 or CD10 expression in Dukes' C and D tumors was higher than that in Dukes' A and B tumors, but there were no significant differences (Fig. 3b,c).

P1, MUC1 and CD10 expression in primary CRC with or without liver metastases

The frequency of P1-positive expression in the primary CRC with synchronous liver metastasis was lower than that without liver metastasis. Conversely, MUC1- and CD10-positive expression in the primary CRC with synchronous liver metastasis were higher than that without liver metastasis. However, there were no significant differences between them (Fig. 4).

Interestingly, the frequency of P1-positive expression in the primary CRC with metachronous liver metastasis was significantly lower than that without liver metastasis ($P < 0.01$; Fig. 4a). The frequency of MUC1- or CD10-positive expression in the primary CRC with metachronous liver metastasis tended to be higher, but there were no significant differences, respectively (Fig. 4b,c).

We examined the P1 staining between primary and metastatic liver tumors, including nine synchronous and four metachronous cases (Table 3). Three tumors had no P1 staining in primary tumors nor in metastatic sites (cases 1, 10, 11). One tumor had P1-negative staining in the primary tumor and the P1-positive area of the metastatic site occupied 12% (case 9). The other nine tumors had a P1-positive area of primary tumors from 2% to 44% and P1-negative staining in the metastatic sites.

Prognosis for lack of liver metastases at the time of primary CRC resection

Retrospectively, the survival rate of 34 patients without liver metastasis at the time of the primary CRC resection was analyzed. The primary CRC was positive for P1 staining in 21 cases and negative in 13 cases. The survival rate in P1-negative cases tended to be worse than that in P1-positive cases ($P = 0.057$; Fig. 5a). The expression of MUC1 or CD10 did not have any relationship with survival rate (Fig. 5b,c).

Table 3 Immunohistochemical expression of P1 in primary and metastatic liver tumors

ID no.	Primary site (%)	Metastasis site (%)
Synchronous liver metastasis		
1	0	0
2	2	0
3	2	0
4	5	0
5	8	0
6	12	0
7	30	0
8	44	0
9	0	12
Metachronous liver metastasis		
10	0	0
11	0	0
12	2	0
13	8	0

Positive expression of P1 in tumor area represents the percentage.

HNF4α expression in colon cancer cell lines

A distinct single band at approximately 52 kDa was detected in a well-differentiated cell line, Caco2, with K9218 (P1).

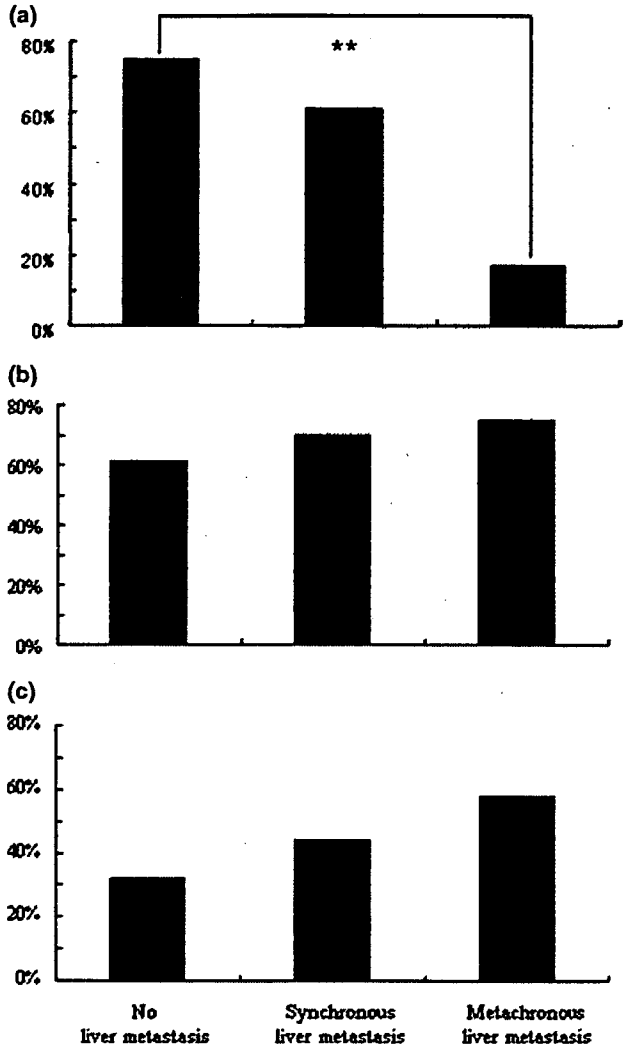

Figure 4 Expression of each marker in primary colorectal carcinoma (CRC) and liver metastasis. (a) The frequency of P1-positive expression in the primary CRC with liver metastasis was lower than that without liver metastasis. While there was no significant relationship between lack of liver metastasis, and presence of synchronous metastasis, there was a significant difference between lack of liver metastasis and presence of metachronous metastasis (no liver metastasis, 21/28, 75%; synchronous liver metastasis, 14/23, 61%; metachronous liver metastasis, 2/12, 17%). (b,c) The frequency of (b) MUC1- or (c) CD10-positive expression in the primary CRC with synchronous or metachronous liver metastasis tended to be higher, but there were no significant differences, respectively. $^{**}P < 0.01$.

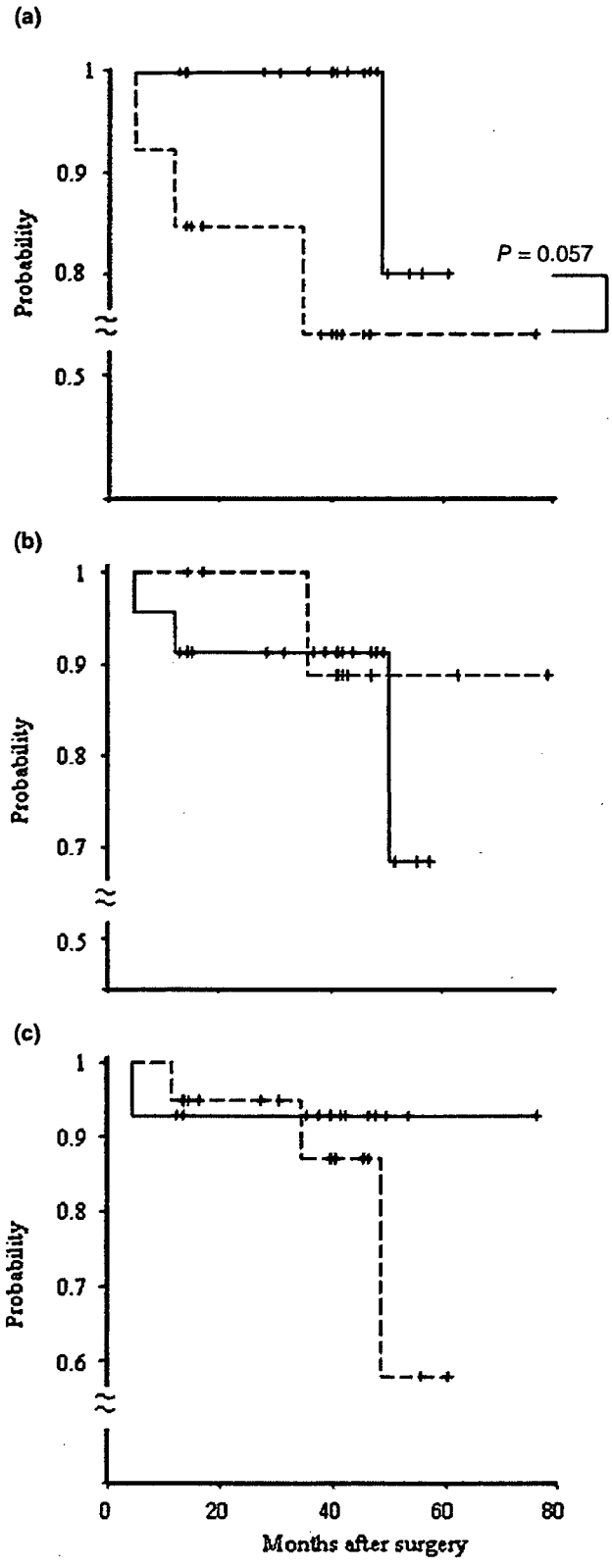

Figure 5 Kaplan-Meier survival curves. Relationships between post-surgical survival outcome and expression of each marker are shown. (a) The survival rate in the (- - -) 13 P1-negative cases tended to be lower than that in the (—) 21 P1-positive cases. The expression of (b) MUC1 (—, positive; - - -, negative) or (c) CD10 (—, positive; - - -, negative) did not show any relationship with survival rate.

Other progressive human colon cancer cell lines had no band (Fig. 6). A single band at approximately 48 kDa was detected in each cancer cell line with H6939 (P2). Two bands corresponding to 48 and 52 kDa were detected in Caco2, and shorter bands were detected in other cancer cell lines with H1415 (P1/P2).

DISCUSSION

Liver metastasis is the most critical prognostic factor for CRC. The early stage detection of liver metastasis is most important for improving patient survival. Recently, MUC1 and CD10 have received attention as useful markers that could predict metastasis in CRC. It is known that MUC1-positive expression in CRC is distinctly related to tumor progression.[4,7,8] It is known that CD10-positive expression is related to venous invasion and liver metastasis.[9,10] In the present study MUC1 expression was significantly different only with respect to depth of tumor invasion. We could not find any relationships between CD10 expression and tumor characteristics. To our knowledge, the relationship between HNF4α and CRC has not been fully examined. The frequency of P1-positive expression in CRC with metastasis (Dukes' C and D) was significantly lower than that without metastasis (Dukes' A and B). The frequency of P1-positive expression in CRC with metachronous liver metastasis was significantly lower than that without liver metastasis. These findings indicate that downregulated P1 expression is involved in the progression of carcinoma from the non-metastatic to the metastatic stage. The survival rate in P1-negative cases tended to be worse than that in P1-positive cases. In comparison to P1 expression between 13 primary and metastatic tumors, P1 expression in metastatic sites was negative, except in one case. This case had P1-negative staining in a primary site and the P1-positive area of the metastatic site occupied 12%. This difference may occur due to deviation of the phenotype of the carcinoma in the liver site. Nine P1-expressive primary tumors had no P1 staining in the metastatic sites. These findings indicate that the P1-negative component in the primary tumors may have disseminated. In the examination of human colon cancer cell lines, well-differentiated adenocarcinoma-derived Caco2 was detected to have P1 protein. P1 protein was not detected in the progressive cancer cell line-derived DLD-1. A decrease of P1 expression was related with an undifferentiated histological stage.

In the present study there was a distinct relationship between P1 expression and metastases, but the role of P1 in metastases remains unsolved. Chiba *et al.* reported that the expression of P1 led to the translocation of tight-junction (TJ) proteins, including occludin, claudin-6 and claudin-7.[19] It is widely accepted that the loss of cell-to-cell adhesion by the loss of TJ proteins is an early event in the process of metastasis.[20,21] Occludin was the first identified as TJ-associated transmembrane protein.[22] During tumor progression, the loss of occludin may lead to the loss of membrane polarity.[23] The expression of occludin progressively decreases in parallel with the increasing grade of human endometrial carcinoma,[24] and in parallel with the loss of differentiation in gastrointestinal adenocarcinomas.[23] Claudins are also essential for TJ, constituting more than 20 members of a gene family in mice and humans. The loss of claudin proteins has been observed in colon cancer,[25] hepatocellular carcinoma,[26] thyroid cancer[27] and breast cancer.[28] We evaluated the expression of occludin and claudin-7 in the present series, in order to investigate whether the altered expressions of these proteins are associated with P1 immunoreactivity. However, there was no association with these proteins and P1 (data not shown). E-cadherin is known to be an adhesion protein, and its expression is lower with respect to the de-differentiation of CRC.[29] However, the relation between E-cadherin and tumor invasion, and metastasis is still not clear.[30] HNF4α is known to directly activate expression of the *HNF1α* gene.[31] Recently, Sakaguchi *et al.* have shown that HNF1α induces claudin-2 expression.[32] In this sense, the downregulation of HNF4α may affect the expression of claudins.

In conclusion, the present study indicates that P1 could be a novel useful marker for metachronous liver metastasis and prognosis in CRC. Further prospective studies should be performed to evaluate the predictive ability of P1 for precise survival rate and prognosis.

ACKNOWLEDGMENTS

The authors thank Mr S. Momozaki, K. Oyauchi and T. Aoyama (Division of Cellular and Molecular Pathology, Department of Cellular Function, Niigata University Graduate School of Medical and Dental Science) for their excellent technical assistance. This study was supported by the Program of Fundamental Studies in Health Sciences of the National Institute of Biomedical Innovation (NIBIO), by the Focus 21 project of the New Energy and Industrial Technology Development Organization (NEDO), and by the Special Coordination Fund for Science and Technology from the Ministry of Education, Culture, Sports, Science and Technology.

REFERENCES

1 National Cancer Center Japan. *Cancer Statistics in Japan.* Tokyo: National Cancer Center Japan, 2005. Available from URL: http://www.ncc.go.jp/jp/statistics/2005/index.html (accessed December 2005).
2 Almersjo O, Bengmark S, Hafstrom L. Liver metastases found by follow-up of patients operated on for colorectal cancer. *Cancer* 1976; **37**: 1454–7.
3 Baba H, Watanabe O, Itano O *et al.* Clinicopathological analysis of liver metastasis from colorectal cancer. *J Jpn Soc Coloproctol* 1999; **52**: 169–78.
4 Nakamori S, Ota DM, Cleary KR, Shirotani K, Irimura T. MUC1 mucin expression as a marker of progression and metastasis of human colorectal carcinoma. *Gastroenterology* 1994; **106**: 353–61.
5 McGuckin MA, Walsh MD, Hohn BG, Ward BG, Wright RG. Prognostic significance of MUC1 epithelial mucin expression in breast cancer. *Hum Pathol* 1995; **26**: 432–9.
6 Higashi M, Yonezawa S, Ho JJ *et al.* Expression of MUC1 and MUC2 mucin antigens in intrahepatic bile duct tumors: Its relationship with a new morphological classification of cholangiocarcinoma. *Hepatology* 1999; **30**: 1347–55.
7 Matsuda K, Masaki T, Watanabe T *et al.* Clinical significance of MUC1 and MUC2 mucin and P53 protein expression in colorectal carcinoma. *Jpn J Clin Oncol* 2000; **30**: 89–94.
8 James CB, Robert SB. Mucinous and mucin binding proteins in colorectal cancer. *Cancer Metastasis Rev* 2004; **23**: 77–99.
9 Yao T, Tsutsumi S, Akaiwa Y *et al.* Phenotypic expression of colorectal adenocarcinoma with reference to tumor development and biological behavior. *Jpn J Cancer Res* 2001; **92**: 755–61.
10 Yao T, Takata M, Tsutsumi S *et al.* Phenotypic expression of gastrointestinal differentiation markers in colorectal adenocarcinomas with liver metastasis. *Pathology* 2002; **34**: 556–60.
11 Sladek FM, Zhong WM, Lai E, Darnell JE. Liver-enriched transcription factor HNF-4 is a novel member of the steroid hormone receptor superfamily. *Genes Dev* 1990; **4**: 2353–65.
12 Jiang G, Nepomuceno L, Hopkins K, Sladek FM. Exclusive homodimerization of the orphan receptor hepatocyte nuclear factor 4 defines a new subclass of nuclear receptors. *Mol Cell Biol* 1995; **15**: 5131–43.
13 Sladek FM. Orphan receptor HNF-4 and liver-specific gene expression. *Receptor* 1993; **3**: 223–32.
14 Jiang S, Tanaka T, Iwanari H *et al.* Expression and localization of P1 promoter-driven hepatocyte nuclear factor-4α (HNF4α) isoforms in human and rats. *Nucleic Recept* 2003; **1**: 1–12.
15 Tanaka T, Jiang S, Hotta H *et al.* Dysregulated expression of P1 and P2 promoter-driven hepatocyte nuclear factor-4α in the pathogenesis of human cancer. *J Pathol* 2006; **208**: 662–72.
16 Sel S, Ebert T, Ryffel GU, Drewes T. Human renal cell carcinogenesis is accompanied by a coordinate loss of the tissue specific transcription factors HNF4α and HNF1α. *Cancer Lett* 1996; **101**: 205–10.
17 Lazarevich NL, Cheremnova OA, Varga EV *et al.* Progression of HCC in mice is associated with a downregulation in the expression of hepatocyte nuclear factors. *Hepatology* 2004; **39**: 1038–47.
18 Saito T, Yamamoto T, Kazawa T, Gejyo H, Naito M. Expression of toll-like receptor 2 and 4 in lipopolysaccharide-induced lung injury in mouse. *Cell Tissue Res* 2005; **321**: 75–88.
19 Chiba H, Gotoh T, Kojima S *et al.* Hepatocyte nuclear factor (HNF)-4α triggers formation of functional tight junctions and establishment of polarized epithelial morphology in F9 embryonal carcinoma cells. *Exp Cell Res* 2003; **286**: 288–97.

20 Mori M, Sawada N, Kokai Y, Satoh M. Role of tight junctions in the occurrence of cancer invasion and metastasis. *Med Electron Microsc* 1999; **32**: 193–8.
21 Mortin TA, Jiang WG. Tight junctions and their role in cancer metastasis. *Histol Histopathol* 2001; **16**: 1183–95.
22 Furuse M, Hirase T, Itoh M, Nagafuchi A, Yonemura S, Tsukita S. Occludin: A novel integral membrane protein localizing at tight junctions. *J Cell Biol* 1993; **123**: 1777–88.
23 Tobioka H, Isomura H, Kokai Y, Sawada N. Polarized distribution of carcinoembryonic antigen is associated with a tight junction molecule in human colorectal adenocarcinoma. *J Pathol* 2002; **198**: 207–12.
24 Tokunaga Y, Tobioka H, Isomura H, Kokai Y, Sawada N. Expression of occludin in human rectal carcinoid tumors as a possible marker for glandular differentiation. *Histopathology* 2004; **44**: 247–50.
25 Soler AP, Miller RD, Laughlin KV, Carp NZ, Klurfeld DM, Mullin JM. Increased tight junctional permeability is associated with the development of colon cancer. *Carcinogenesis* 1999; **20**: 1425–31.
26 Swift JG, Mukherjee TM, Rowland R. Intercellular junctions in hepatocellular carcinoma. *J Submicrosc Cytol* 1983; **15**: 799–810.
27 Cochand-Priollet B, Raison D, Molinie V, Guillausseau PJ, Wassef M, Bouchaud C. Altered gap and tight junctions in human thyroid oncocytic tumors: A study of 8 cases by freeze-fracture. *Ultrastruct Pathol* 1998; **22**: 413–20.
28 Kramer F, White K, Kubbies M, Swisshelm K, Weber BH. Genomic organization of claudin-1 and its assessment in hereditary and sporadic breast cancer. *Hum Genet* 2000; **107**: 249–56.
29 van der Wurff A, ten Kate J, van der Linden EP, Dinjens WN, Arends JW, Bosman FT. L-CAM expression in normal, premalignant, and malignant colon mucosa. *J Pathol* 1992; **168**: 287–91.
30 van der Wurff AA, Arends JW, van der Linden EP, ten Kate J, Bosman FT. L-CAM expression in lymph node and liver metastases of colorectal carcinomas. *J Pathol* 1994; **172**: 177–81.
31 Tian JM, Schibler U. Tissue-specific expression of the gene encoding hepatocyte nuclear factor 1 may involve hepatocyte nuclear factor 4. *Genes Dev* 1991; **5**: 2225–34.
32 Sakaguchi T, Gu X, Golden HM, Suh E, Rhoads DB, Reinecker HC. Cloning of the human claudin-2 5′-flanking region revealed a TATA-less promoter with conserved binding sites in mouse and human for caudal-related homeodomain proteins and hepatocyte nuclear factor-1α. *J Biol Chem* 2002; **277**: 21 361–70.

Journal of Viral Hepatitis, 2008, 15, 293–299 doi:10.1111/j.1365-2893.2007.00943.x

Economic impact of extended treatment with peginterferon α-2a and ribavirin for slow hepatitis C virologic responders

J. Nakamura,[1] S.-I. Toyabe,[1] Y. Aoyagi[2] and K. Akazawa[1] *Divisions of [1]Information Science and Biostatistics and [2]Gastroenterology and Hepatology, Niigata University Graduate School of Medical and Dental Sciences, Niigata, Japan*

Received 11 June 2007; accepted for publication 10 August 2007

SUMMARY. It is difficult to achieve a sustained virologic response from antiviral therapy for genotype 1 hepatitis C virus-infected patients without a sufficient virologic response in the early weeks after treatment. However, a recent study has reported on the effectiveness of an extended course of treatment with peginterferon α-2a plus ribavirin for slow virologic responders. The aim of this study was to evaluate the economic impact of an extended course of treatment. A Markov cohort model of hepatitis C was designed in order to demonstrate the clinical states, based on the assigned transition probabilities over 30 years. The slow virologic responders treated with an extended 72-week course of therapy could increase by 0.55 the quality-adjusted life years (=15.35–14.80) and reduce the lifetime cost by $2762 (=71 559–69 438) in comparison with those treated by the standard 48-week course. One-way sensitivity analyses did not change the cost-effectiveness. Therefore, the extended 72 weeks of treatment with peginterferon α-2a plus ribavirin for slow virologic responders could be cost-effective in comparison with the standard 48 weeks of treatment.

Keywords: combination therapy, economic impact, extended treatment, peginterferon, ribavirin, slow virologic responders.

INTRODUCTION

The World Health Organization estimates that approximately 180 million people are infected with the hepatitis C virus (HCV), of whom 130 million are at risk of progressing to liver cirrhosis and/or hepatocellular carcinoma. It is also estimated that 3 to 4 million people are newly infected with HCV each year, 70% of whom will develop chronic hepatitis. The incidence of hepatocellular carcinoma (HCC) and the mortality from HCC have been increasing and approximately 50–76% of HCC cases are derived from HCV [1]. The age-adjusted incidence of HCC per 10 000 in Western Europe was reported to be 4.89 in men and 1.55 in women [2].

In the 1990s, interferon monotherapy was the primary treatment used to eradicate HCV from infected patients. When patients achieved a sustained virologic response with interferon, their risk of having HCC in their lifetime became very small. Recently, peginterferon in combination with ribavirin has proved to be more effective than interferon alone or interferon in combination with ribavirin [3,4]. The sustained virologic response (SVR) rate in genotype 1-infected patients treated with peginterferon α-2a plus ribavirin has been reported to be 46%, which was significantly higher than the SVR rate of 36% in patients treated with interferon α-2b plus ribavirin [4].

In the previous cost-effectiveness analyses of the treatment with peginterferon plus ribavirin, genotype 1-infected patients without an early virologic response at week 12 after treatment were excluded from the analyses because of the low possibility of achieving SVR with additional treatment [5,6]. However, a recent report suggested that patients with a slow virologic response, defined as detectable HCV-RNA at week 12 but negative at week 24, could reach SVR to some extent if the treatment duration was extended to 72 weeks. A randomized clinical trial, which included 455 patients, was conducted by Berg *et al.*, in which 230 patients were assigned to a standard 48-week regimen, while the other 225 patients received an extended 72-week regimen [7]. It was demonstrated that those genotype 1-infected patients with a slow virologic response could achieve a 29% SVR rate following 72 weeks of treatment (extended protocol) with peginterferon α-2a plus ribavirin. This SVR rate was significantly higher than the 17% SVR demonstrated in the patients treated for the standard 48-week regimen (standard protocol). They also indicated that the 40% relapse rate of patients treated by the extended protocol was significantly lower than the 64% relapse rate occurring with the standard

Abbreviations: HCC, hepatocellular carcinoma; HCV, hepatitis C virus; LE, life expectancy; QALYs, quality adjusted life years; SVR, sustained virologic response.

Correspondence: Junichiro Nakamura, 1-754 Asahimachi-dori, Chuo-ku, Niigata 951-8520, Japan. Tel.: +81 25 227 2472; Fax: +81 25 227 0850; E-mail: ichirojn@med.niigata-u.ac.jp

protocol. However, it is not known whether the extended protocol is cost-effective or not.

The aim of this study was to assess the economic impact of the extended protocol for patients with a slow virologic response to treatment with peginterferon α-2a and ribavirin, in genotype 1-infected chronic hepatitis C patients.

MATERIALS AND METHODS

Model

A Markov cohort model was designed in order to assess the economic impact of the extended protocol in genotype 1 HCV-infected patients (Fig. 1). The Markov cohort model begins in the initial state and the patients remain in the same state or transfer to a possible subsequent state, according to the transition probabilities at each cycle [8,9]. As shown in Fig. 1, our model has six Markov states which are denoted by circles, and the rectangles show the terminal state or namely death. When the Markov cohort analysis is stopped at a projected endpoint, the total number of patient-cycles for each state is divided by the size of the original cohort. Finally, the expected time and the cost that each patient will incur in each state are added in order to evaluate the cost-effectiveness. The life expectancy (LE) and the lifetime cost could be calculated in this way. In our model, the standard protocol, the extended protocol and no treatment strategy were analysed.

Assumption

The treatment regimen, based on the randomized clinical trial by Berg *et al.*, is described in Fig. 2 [7]. The HCV-RNA level was monitored by real-time reverse transcription-polymerase chain reaction. An SVR was defined as being serum HCV-RNA negative both at the end of treatment and

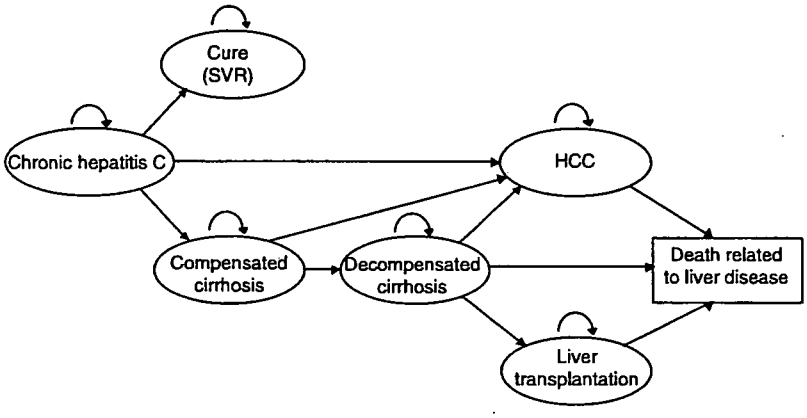

Fig. 1 Structure of the Markov cohort model in hepatitis C for the cost-effectiveness analysis.

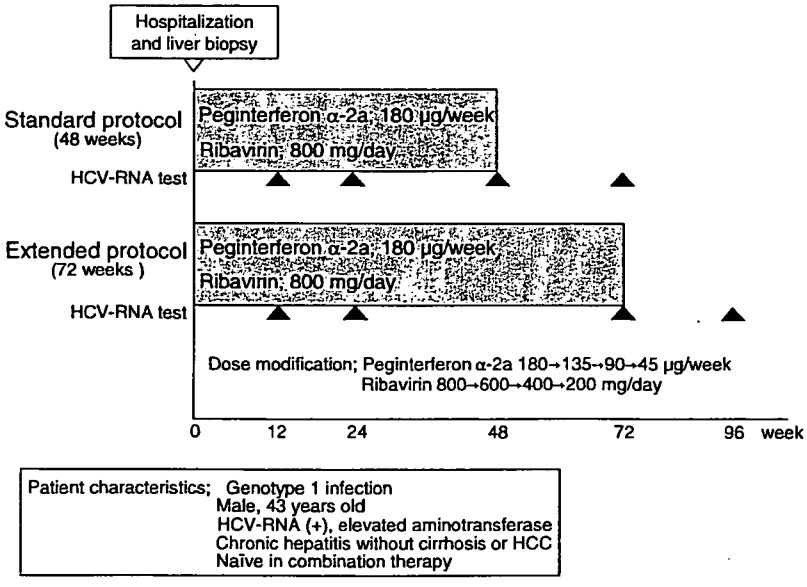

Fig. 2 The regimen for the combination therapy with peginterferon α-2a and ribavirn incorporated in the model.

after 24 weeks of follow-up. The patients were considered to be 43-year-old males with chronic hepatitis C and the age was the mean in the randomized clinical trial [7]. Their other characteristics are also demonstrated in Fig. 2. They were assumed to have discontinued their treatment when their HCV-RNA levels did not decrease by less than 2 $\log_{10}$ from the pretreatment levels at week 24. The patients who relapsed after treatment or those patients who discontinued treatment, were not treated again and received no benefit from the combination therapy. The Markov cohort analysis was performed for up to 30 years of the patients' lifetime.

Model parameters

A literature search was performed in order to estimate the annual transition probabilities of the progression to subsequent states (Table 1) [10–25]. The literature was searched using Medline for studies published up to March 2007. The following MeSH terms and their combinations were used for searching: hepatitis C, chronic, fibrosis, carcinoma, hepatocellular, survival, liver transplantation and follow-up studies. The rates of SVR and discontinuation, incorporated in our model, were based on the aforementioned randomized controlled trial (Table 1) [7]. The age-specific death rates for the general population were estimated from the abridged life table for Japan in 2004 [26]. The inpatient costs were derived from the actual data on the patients with decompensated cirrhosis and HCC. The outpatient costs included the costs for hospital visits, laboratory tests, ultrasonography, radiography and for the other medical procedures which were needed for the state in our model. As shown in Table 2, the costs for liver transplantation were obtained from published sources [6,22,27]. When estimating the cost for each state, only the direct health-care costs were considered. All of the costs were converted into US dollars using the 2006 exchange rates as reported by the Organization for Economic Co-operation and Development (OECD) (Table 2) [28]. For decompensated cirrhosis, the three states considered were those with ascites, variceal bleeding or encephalopathy. The rates of the three states were taken from the two prospective studies and they were assumed to be 76.0, 18.5 and 5.5%, respectively [15,29]. The estimated values, which reflected the quality of life at the various states related to chronic hepatitis C, were assigned and the quality-adjusted life years (QALYs) was the sum of the values. The values for the health-related quality of life, varying from 0 (death) to 1 (perfect health), were taken from previously published sources (Table 2) [30].

Cost-effectiveness analysis

The cost-effectiveness during the 30-year follow-up period for the patients was evaluated by calculating the lifetime cost, the life expectancies (LEs) and the QALYs. These values in the cost-effectiveness analysis were compared with the values obtained from the patients with a slow virologic response when treated by the standard protocol and the extended protocol.

First, a base-case analysis was performed by incorporating the baseline parameters which were shown in Tables 1 and 2 in the model. Next, a one-way sensitivity analysis was performed by varying the parameters which were likely to change the lifetime cost, LEs and QALYs. The parameters, such as treatment effectiveness (i.e. SVR) and the transition

Table 1 Treatment effectiveness (SVR) and transition probabilities incorporated in the model

	Base	Range	Reference
SVR rate			
Standard protocol (48 weeks of treatment)	0.17	0.09–0.24	7
Extended protocol (72 weeks of treatment)	0.29	0.20–0.37	7
Transition probability			
Chronic hepatitis to compensated cirrhosis	0.065	0.044–0.091	10,11
Chronic hepatitis to HCC	0.014	0.007–0.020	12,13
Compensated cirrhosis to decompensated cirrhosis	0.029	0.018–0.041	14,15
Compensated cirrhosis to HCC	0.073	0.055–0.093	12–15, 16–21
Decompensated cirrhosis to HCC	0.073	0.055–0.093	12–15, 16–21
Decompensated cirrhosis to liver transplantation	0.031	0.01–0.05	22
Decompensated cirrhosis to death	0.153	0.012–0.186	21
HCC to death	0.194	0.192–0.196	23,24
Liver transplantation to death (first year)	0.136	0.126–0.146	25
Liver transplantation to death (subsequent years)	0.052	0.048–0.055	25

Probable ranges of the SVR rate. Almost all of the transition probabilities were based on their 95% confidence interval. The range of the transition probability from decompensated cirrhosis to liver transplantation was estimated from expert opinions. HCC, hepatocellular carcinoma; SVR, sustained virologic response.